Theories of Sunspot Formation: State of the Art

I. ROGACHEVSKII, N. KLEEORIN,

Ben-Gurion University of the Negev, Beer Sheva, Israel

NORDITA, KTH Royal Institute of Technology and Stockholm University, Sweden

A. BRANDENBURG, Dh. MITRA, K. KEMEL, P. KÄPYLÄ, M. KÄPYLÄ
J. WARNECKE*, I.R. LOSADA, S. JABBARI

NORDITA, KTH Royal Institute of Technology and Stockholm University,
and Department of Astronomy, Stockholm University, Sweden
**Max-Planck-Institut für Sonnesystemforschung, Göttingen, Germany*

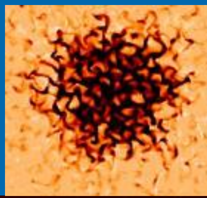

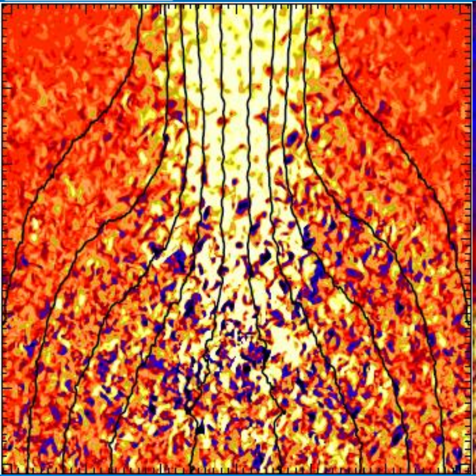

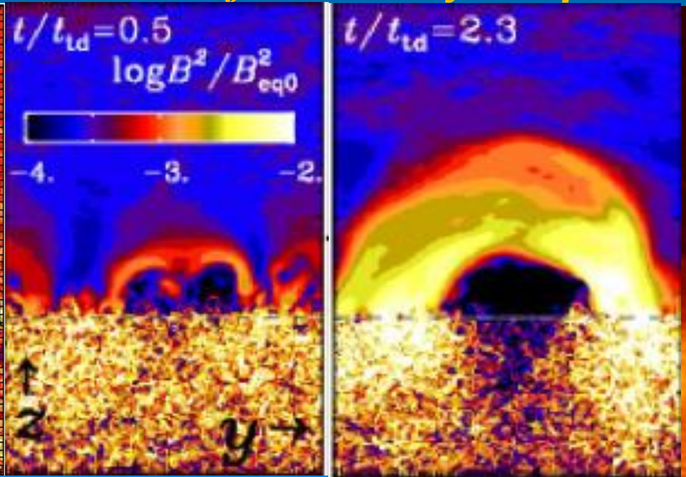

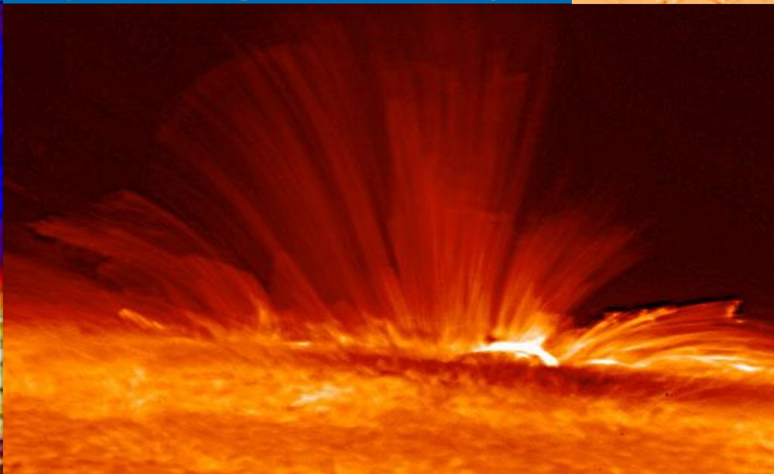

Active regions and Sunspots

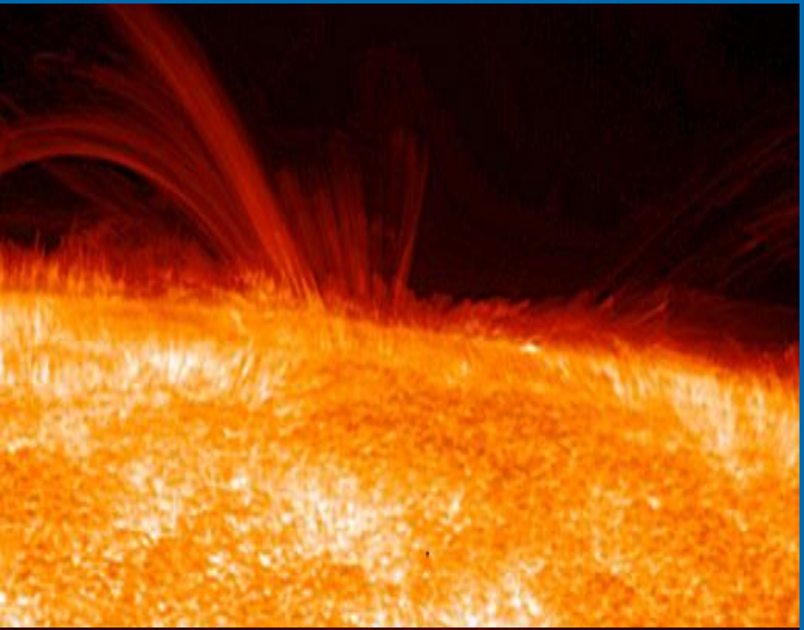

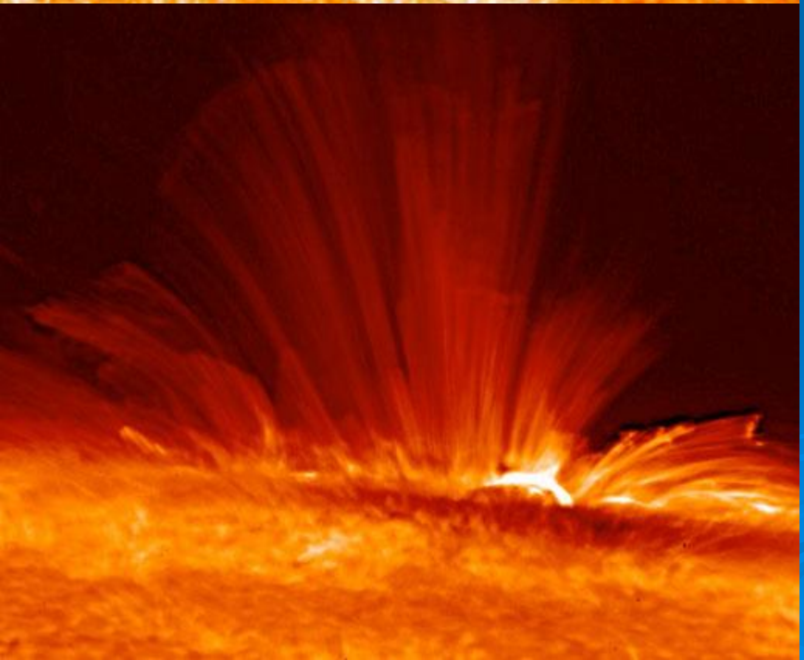

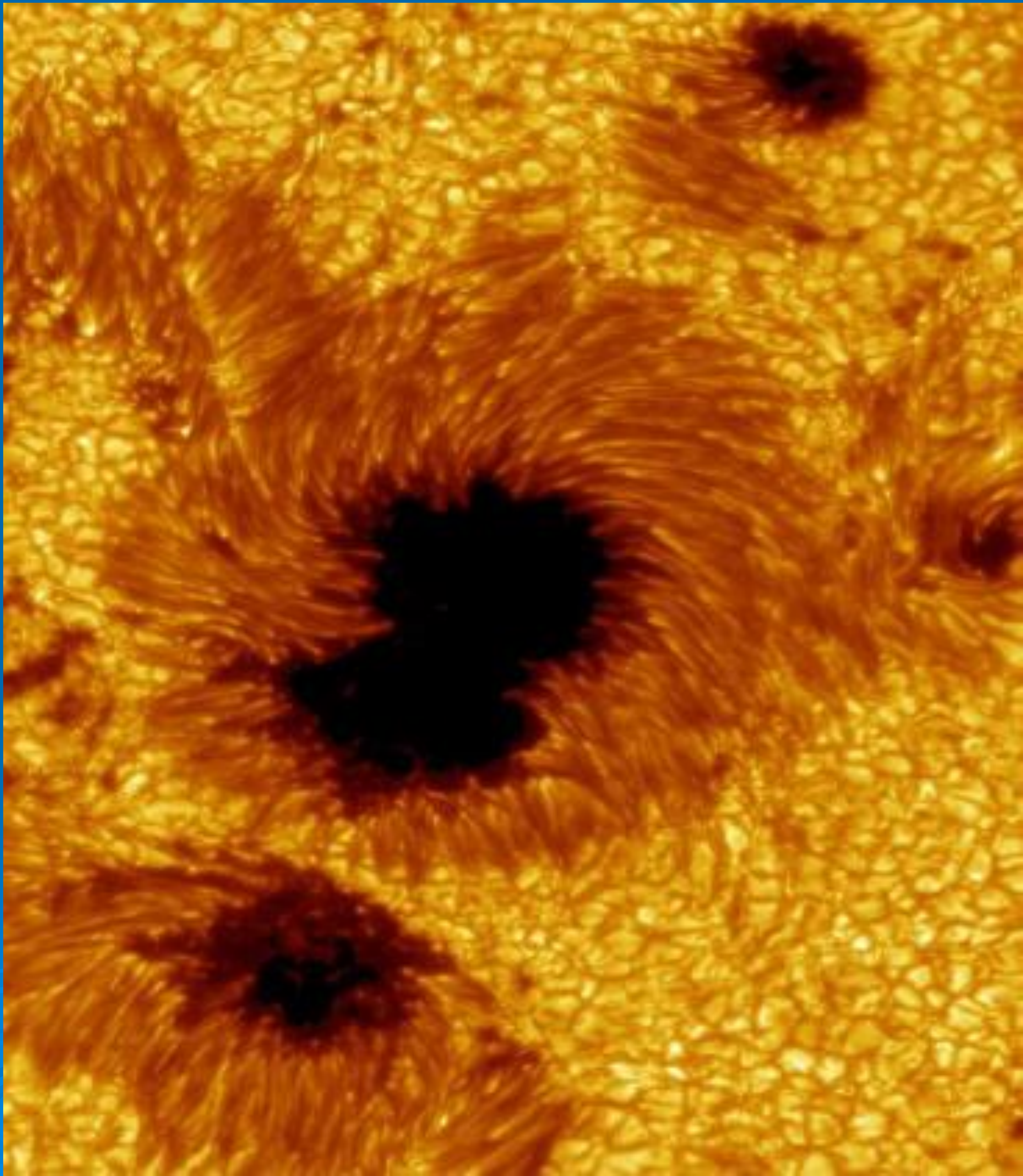

Active regions

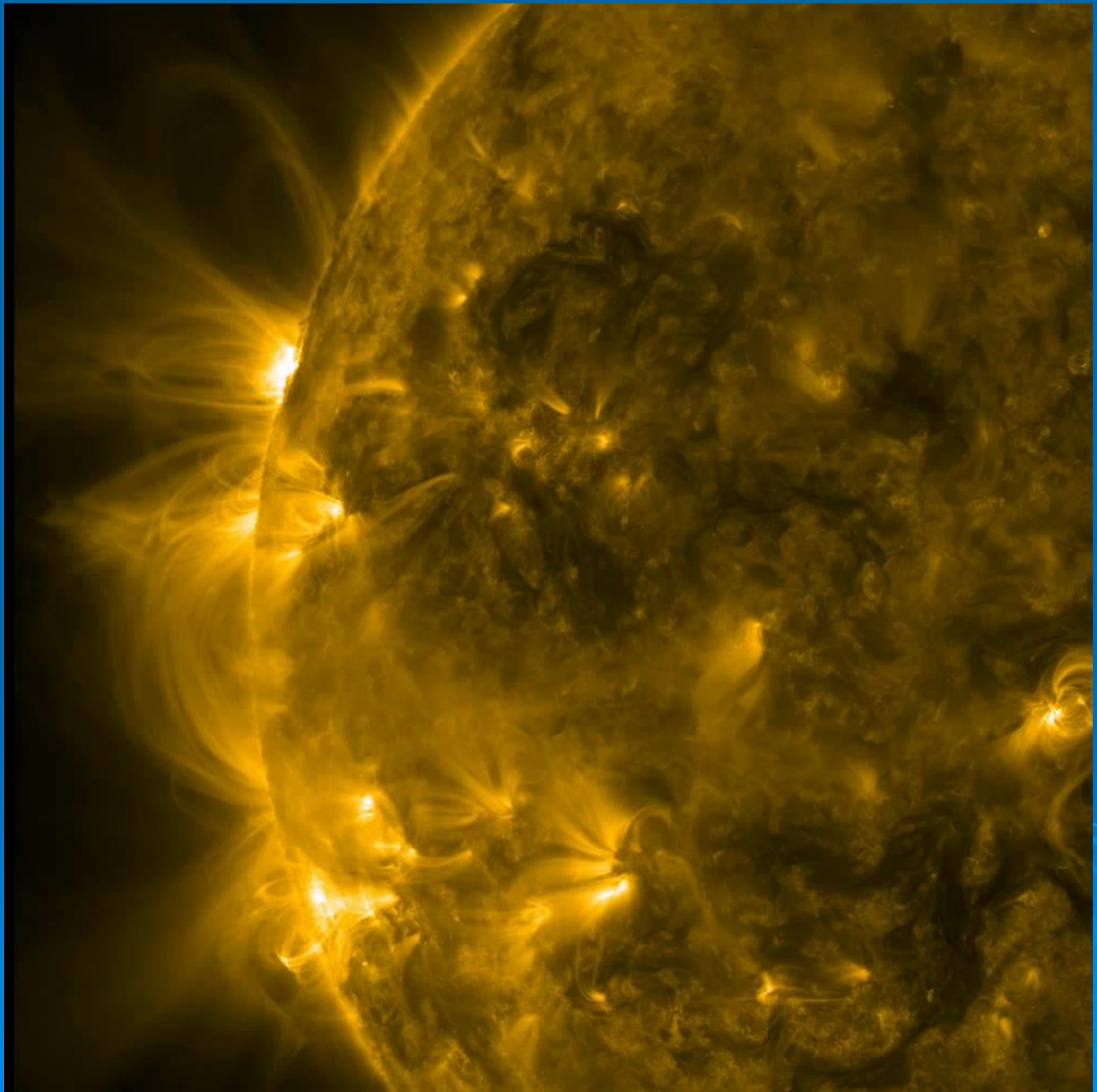

Solar convection

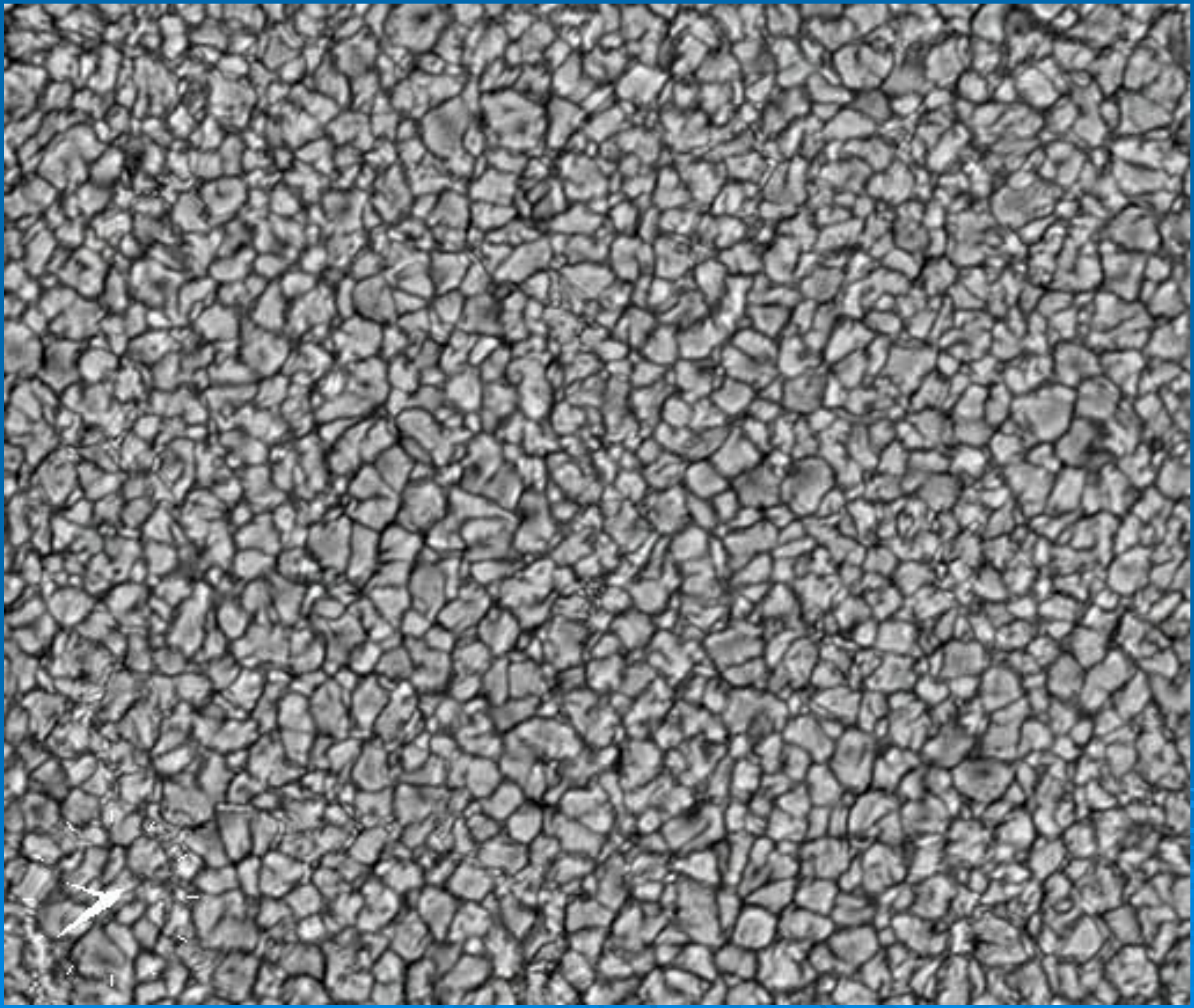

Problems

- **What is the mechanism of formation of solar magnetic structures in turbulent convection zone?**
- **Solar dynamo mechanism can generate only weak (<< 1000G) nearly uniform large-scale magnetic field.**
- **How is it possible to create strongly inhomogeneous magnetic structures from originally uniform magnetic field?**

Theories of Sunspots Formation

1. Flux-Transport Dynamo

- 1). The solar dynamo produces strong magnetic fields at the bottom of the convection zone at the tachocline region (Parker 1975; Spiegel & Weiss 1980; Spiegel & Zahn 1992, Schou et al. 1998), where there is a strong shear layer, that produces strong toroidal magnetic field.
- 2) The field becomes unstable and rises upward in form of flux tubes, which reach the surface of the sun and form bipolar structures and sunspots (Caligari et al. 1995).

Criticism:

- A) However, the field in the tachocline region should be reach $10^5 G$, which is needed for a coherent flux tube to reach the surface without strong distortion (Choudhuri & Gilman 1987; D'Silva & Choudhuri 1993).
- B) The generation of such strong coherent magnetic flux tubes has not yet been seen in self-consistent dynamo simulations (Guerrero & Käpylä 2011; Nelson et al. 2011; Fan & Fang 2014).
- C) Helioseismology also does not support a deeply rooted flux tube scenario (Kosovichev & Stenflo 2008, Stenflo & Kosovichev 2012, Howe et al. 2009; Antia & Basu 2011).

2. Negative Effective Magnetic Pressure Instability (NEMPI)

Outline

- **Physics of the effect of turbulence on large-scale magnetic pressure (on large-scale Lorentz force)**
- **Direct numerical simulations of the effect of turbulence on large-scale Lorentz force**
- **Large-scale instability (NEMPI): numerical simulations and theory**
- **Estimates for the solar convective zone**

Different Effects of Turbulence

- Turbulent viscosity
- Turbulent diffusion
- Turbulent magnetic diffusion
- Alpha effect
- Turbulent diamagnetic or paramagnetic velocity
- Lambda effect – generation of differential rotation
- Turbulent Thermal diffusion

Lorentz Force and Momentum Equation

$$\mathbf{J}\times\mathbf{B} = (\boldsymbol{\nabla}\times\mathbf{B})\times\mathbf{B} = -\boldsymbol{\nabla}\frac{\mathbf{B}^2}{2}+(\mathbf{B}\cdot\boldsymbol{\nabla})\mathbf{B} = -\nabla_j\left[\frac{1}{2}\boldsymbol{B}^2\delta_{ij} - B_iB_j\right]$$

$$\frac{\partial}{\partial t}\rho\,\mathbf{U}_i = -\nabla_j\,\Pi_{ij}$$

where

$$\Pi_{ij} = \rho\,U_iU_j + \delta_{ij}\,(p+\frac{1}{2}\mathbf{B}^2) - B_iB_j - \sigma^{\nu}_{ij}(\mathbf{U}) + \ldots$$

Averaged equation: $\mathbf{U} = \bar{\mathbf{U}} + \mathbf{u}\,,\qquad \mathbf{B} = \bar{\mathbf{B}} + \mathbf{b}$

$$\frac{\partial}{\partial t}\bar{\rho}\,\bar{\mathbf{U}}_i = -\nabla_j\,\bar{\Pi}_{ij}$$

where

$$\bar{\Pi}_{ij} = \bar{\rho}\,\bar{U}_i\bar{U}_j + \delta_{ij}\,(\bar{p}+\frac{1}{2}\bar{\mathbf{B}}^2) - \bar{B}_i\bar{B}_j - \bar{\sigma}^{\nu}_{ij}(\bar{\mathbf{U}}) + \frac{1}{2}\langle\mathbf{b}^2\rangle\,\delta_{ij} - \langle b_ib_j\rangle + \bar{\rho}\langle u_iu_j\rangle + \ldots$$

DNS: 3D Stratified Forced Turbulence

Effective Mean Magnetic Pressure

(sum of turbulent and non-turbulent contributions)

$$\mathrm{J}\times\mathrm{B} = (\nabla\times\mathrm{B})\times\mathrm{B} = -\nabla\frac{\mathrm{B}^2}{2} + (\mathrm{B}\cdot\nabla)\mathrm{B} = -\nabla_j\left[\frac{1}{2}B^2\delta_{ij} - B_iB_j\right]$$

$$\mathrm{B} = \bar{\mathrm{B}} + \mathrm{b}$$

$$\mathcal{P}_{\rm eff}(\beta) = \tfrac{1}{2}[1 - q_{\rm p}(\beta)]\,\beta^2 \quad \text{versus} \quad \beta \equiv |\overline{\boldsymbol{B}}|/B_{\rm eq}$$

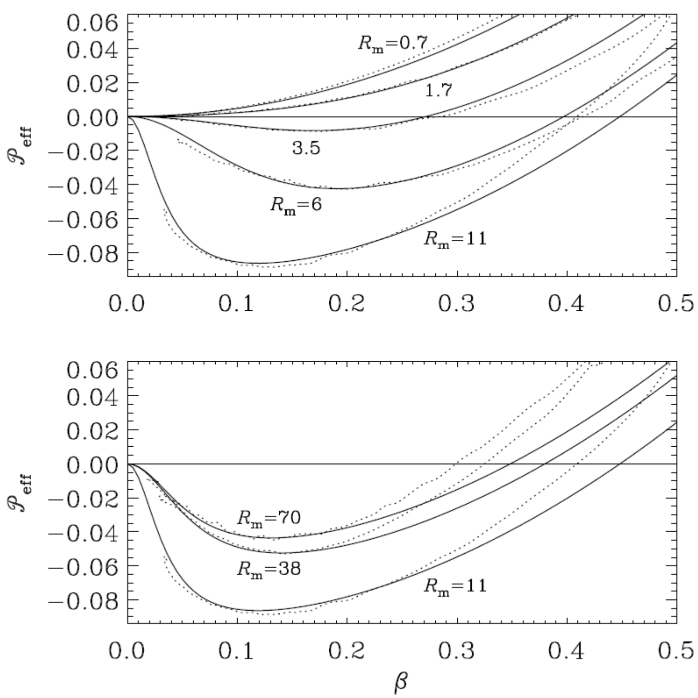

Figure 7. Normalized effective magnetic pressure, $\mathcal{P}_{\rm eff}(\beta)$, for low (upper panel) and higher (lower panel) values of Re_M. The solid lines represent the fits to the data shown as dotted lines.

$$\mathcal{P}_{\rm eff} = \frac{1}{2}(1 - q_p)\frac{\bar{\mathrm{B}}^2}{\mathrm{B}_{\rm eq}^2}$$

Effective magnetic pressure for Rm < 1 is positive, and for Rm > 1, it can be negative.

Quasi-linear theory works only for

$$\mathrm{Rm} \ll 1$$

Equation of State for Isotropic Turbulence

N. Kleeorin, I. Rogachevskii and A. Ruzmaikin,
Sov. Astron. Lett. 15, 274-277 (1989); Sov. Phys. JETP 70, 878-883 (1990)

N. Kleeorin and I. Rogachevskii, ***Phys. Rev. E 50, 2716-2730 (1994)***

I. Rogachevskii and N. Kleeorin, ***Phys. Rev. E 76, 056307 (2007)***

The total turbulent pressure is reduced when magnetic fluctuations are generated

The equation of state for an isotropic turbulence

$$p_T = \frac{1}{3} W_m + \frac{2}{3} W_k \ ,$$

where p_T is the total (hydrodynamic plus magnetic) turbulent pressure,

$W_m = \langle \mathbf{b}^2 \rangle / 2\mu$ is the energy density of the magnetic fluctuations,

$W_k = \rho_0 \langle \mathbf{u}^2 \rangle / 2$ is the kinetic energy density.

Strong reduction of Turbulent Pressure

Magnetic contribution to pressure & energy different!

$$U_iU_j - B_iB_j + \tfrac{1}{2}\delta_{ij}\mathbf{B}^2$$
$$\approx \tfrac{1}{3}\delta_{ij}\left(\mathbf{U}^2 + \tfrac{1}{2}\mathbf{B}^2\right)$$
$$\approx \tfrac{1}{3}\delta_{ij}\left(\underbrace{\mathbf{U}^2 + \mathbf{B}^2}_{\approx const} - \tfrac{1}{2}\mathbf{B}^2\right)$$

Can lead to reversed mean-field buoyancy in *stratified* system

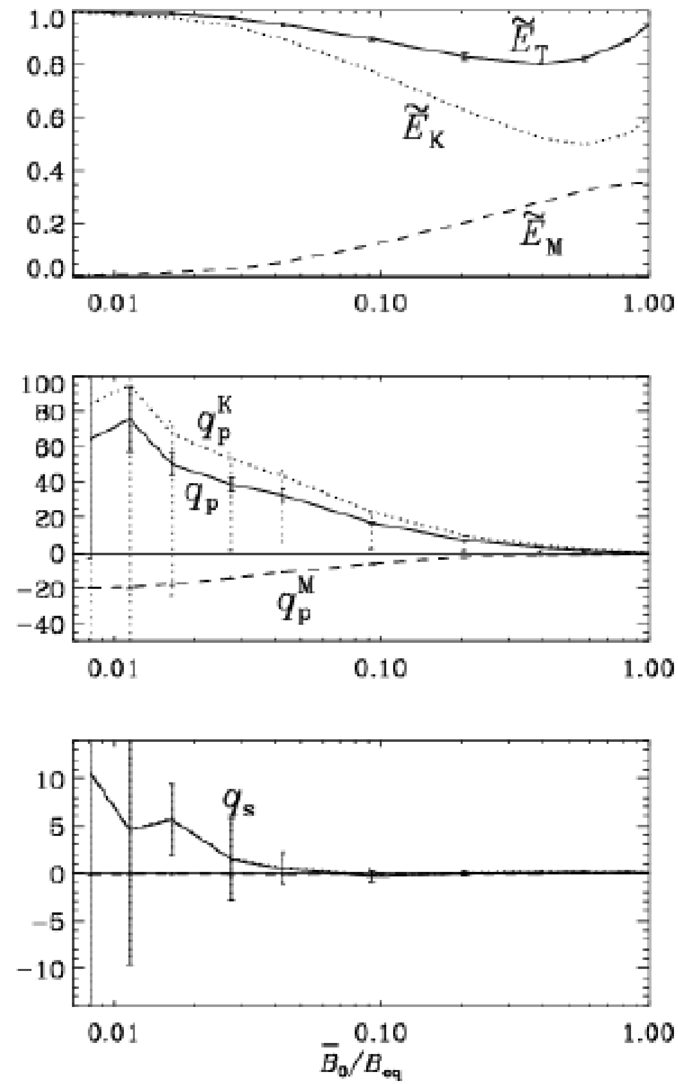

Strong reduction of Turbulent Pressure

Combining the equations:

$$p_T = \frac{1}{3}W_m + \frac{2}{3}W_k = \frac{2}{3}(W_k + W_m) - \frac{1}{3}\mathrm{W_m}\,, \qquad \mathrm{W_k + W_m = const}\,,$$

we can express the change of turbulent pressure δp_T in terms of the change of the magnetic energy density δW_m

$$\delta \mathrm{p_T} = -\frac{1}{3}\delta \mathrm{W_m}$$

Therefore, the turbulent pressure is reduced when magnetic fluctuations are generated (i.e., $\delta \mathrm{W_m} > 0$).

Total Turbulent Energy

The total energy density W_T of the homogeneous turbulence with a nonzero uniform mean magnetic field is conserved

$$\mathrm{W_k + W_m = const.}$$

The uniform large-scale magnetic field performs no work on the turbulence. It can only redistribute the energy between hydrodynamic fluctuations and magnetic fluctuations.

The total energy density $\mathrm{W_T = W_k + W_m}$ of the homogeneous turbulence with a mean magnetic field $\bar{\mathrm{B}}$

$$\frac{\partial W_T}{\partial t} = I_T - \frac{W_T}{\tau_0} + \eta_T \frac{(\boldsymbol{\nabla} \times \bar{\mathrm{B}})^2}{\mu}$$

$I_T =$ is the energy source of turbulence,

W_T/τ_0 determines the dissipation of the turbulent energy.

Equation of State for Anisotropic Turbulence

The equation of state for an anisotropic turbulence

$$p_T = \frac{1}{3(1+\sigma/2)} W_m + \frac{2}{3}\left(\frac{1+3\sigma/4}{1+\sigma/2}\right) W_k \ ,$$

where $0 \leq \sigma < \infty$ is the degree of anisotropy of turbulence.

For a two-dimensional turbulence: $\sigma \to \infty$ and the equation of state reads:

$$p_T = \frac{2}{3\sigma} W_m + W_k = (W_k + W_m) - \mathbf{W_m} \ ,$$

Thus, the change of turbulent pressure δp_T for the two-dimensional turbulence is

$$\delta \mathbf{p_T} = -\delta \mathbf{W_m}$$

Effective Magnetic Pressure

The total pressure is

$$p_{tot} = p_k + p_T + P_B(\bar{B}) ,$$

where p_k is the fluid pressure and $P_B(\bar{B}) = \frac{\bar{\mathrm{B}}^2}{2\mu}$ is the magnetic pressure of the mean field.

Now we examine the part in p_{tot} that depends on the mean (large-scale) magnetic field $\bar{\mathrm{B}}$:

$$\mathrm{P_m}(\bar{\mathrm{B}}) = P_B(\bar{B}) - \mathrm{q_p}(\bar{\mathrm{B}})\frac{\bar{\mathrm{B}}^2}{2\mu} = (1 - \mathrm{q_p}(\bar{\mathrm{B}}))\frac{\bar{\mathrm{B}}^2}{2\mu} \equiv Q_p(\bar{B})\frac{\bar{\mathrm{B}}^2}{2\mu} ,$$

$$p_{\mathrm{tot}} = p + \mathrm{P_m}(\bar{\mathrm{B}}) = p + \mathrm{Q_p}(\bar{\mathrm{B}})\frac{\bar{\mathrm{B}}^2}{2\mu} ,$$

where $p = p_k + p_T^{(0)}$. The pressure $P_m(\bar{B})$ is the combined mean magnetic pressure.

Methods and Approximations

- **Quasi-Linear Approach** or Second-Order Correlation Approximation (SOCA) or First-Order Smoothing Approximation (FOSA)

  Rm << 1 , Re << 1

  Steenbeck, Krause, Rädler (1966); Roberts, Soward (1975)

- **Tau-approaches** (spectral tau-approximation) – **third-order or high-order closure**

  Re >> 1 and Rm >> 1

  Orszak (1970); Pouquet, Frisch, Leorat (1976);
  Kleeorin, Rogachevskii, Ruzmaikin (1990); Rogachevskii, Kleeorin (2007)

- **Renormalization Procedure** (renormalization of viscosity, diffusion, electromotive force and other turbulent transport coefficients) - **Re >> 1 and Rm >> 1 , there is no separation of scales.**

  Moffatt (1981; 1983);
  Kleeorin, Rogachevskii (1994)

Theory: Effective Magnetic Pressure

I. Rogachevskii and N. Kleeorin, *Phys. Rev. E 76, 056307 (2007)*

$$P_m(\bar{B}) = (1 - q_p)\bar{B}^2/\bar{B}_{\rm eq}^2$$

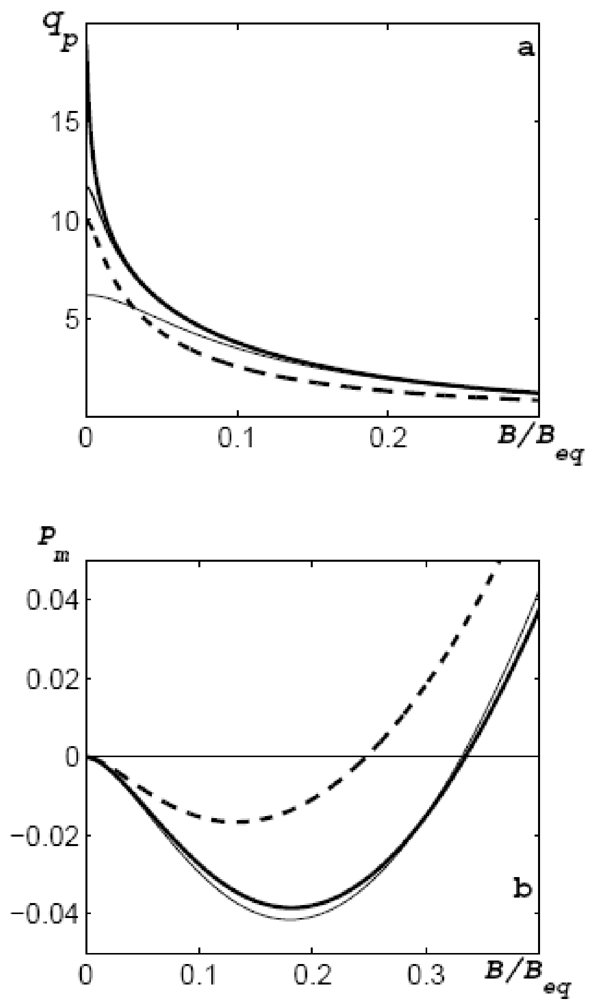

DNS: 3D Forced Non-Stratified Turbulence

A. Brandenburg, N. Kleeorin, I. Rogachevskii, Astron. Nachr. 331, 5-13 (2010)

$$\mathrm{Re} = \frac{u_{rms}}{\nu\, k_f} = 180\,, \qquad \mathrm{Rm} = \frac{u_{rms}}{\eta\, k_f} = 45$$

$$\frac{D\boldsymbol{u}}{Dt} = -\,c_s^2\,\boldsymbol{\nabla}\ln\rho + \frac{\boldsymbol{J}\times\boldsymbol{B}}{\rho} + \boldsymbol{F}_{\rm visc} + \boldsymbol{f},$$

$$k_f = 5\,k_1$$

$$\frac{\partial\,\mathbf{A}}{\partial\,t} = \mathbf{u}\times\mathbf{B} + \eta\boldsymbol{\nabla}^2\mathbf{A}\,,$$

$$\frac{D\,\ln\,\rho}{Dt} = -\,\boldsymbol{\nabla}\cdot\mathbf{u}\,,$$

$$\boldsymbol{B} = \boldsymbol{B}_0 + \boldsymbol{\nabla}\times\boldsymbol{A}$$

All simulations are performed with the PENCIL CODE, which uses sixth-order explicit finite differences in space and a third-order accurate time stepping method.

BOUNDARY CONDITIONS are periodic in 3D.

A white noise non-helical homogeneous and isotropic random forcing.

An isothermal equation of state with constant sound speed: $P = \rho\, c_s^2$

Volume averaging yield: $\langle b_i b_j\rangle,\quad \langle u_i u_j\rangle,$

Effective Lorentz Force - DNS

$$\mathbf{F}^{\mathrm{eff}} = -\frac{1}{2}\boldsymbol{\nabla}(1-q_p)\bar{\mathbf{B}}^2 + (\bar{\mathbf{B}}\cdot\nabla)(1-q_s)\bar{\mathbf{B}}$$

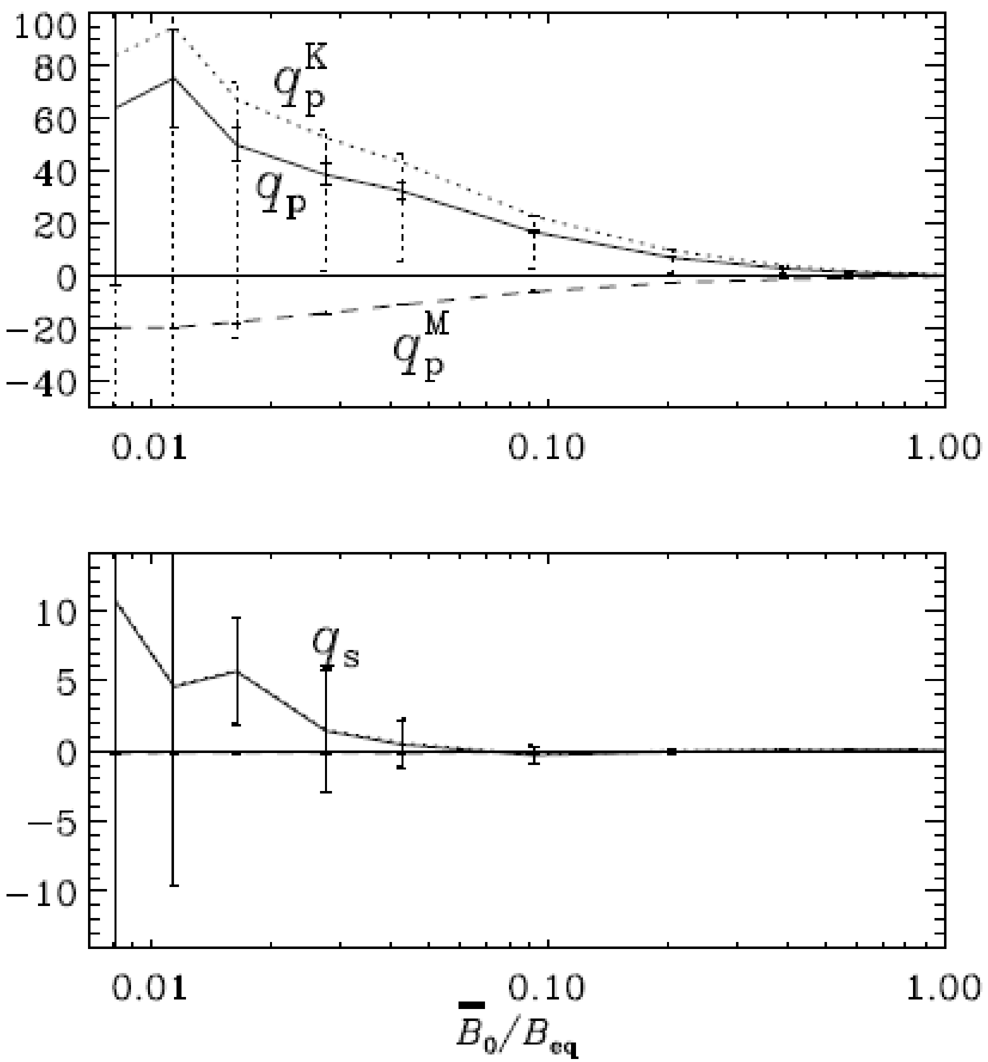

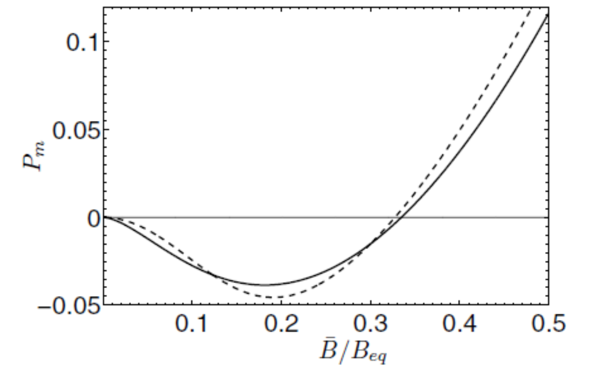

Fig. 3 The effective mean magnetic pressure $P_m(\overline{B}) = (1 - q_p)\overline{B}^2/\overline{B}_p^2$ determined by Rogachevskii & Kleeorin (2007) – solid line, and by the model described by Eq. (26) – dashed line ($\overline{B}_p = 0.21\, c_{s0}\rho_0^{1/2}$ and $q_{p0} = 4$).

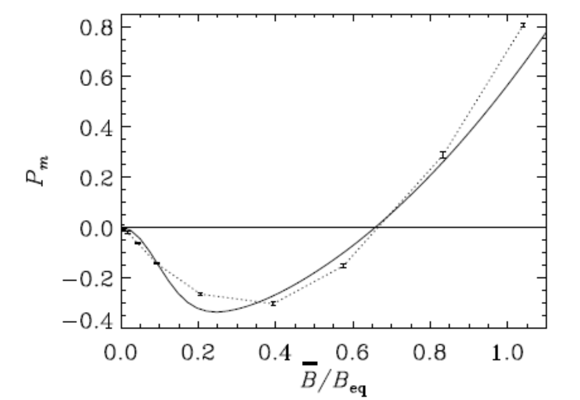

Fig. 4 Same as Fig. 3, but from simulation (dotted line). The solid line shows a fit [Eq. (26)] with $\overline{B}_p = 0.022\, c_{s0}\rho_0^{1/2}$ (corresponding to $\overline{B}_p/B_{eq} = 0.18$) and $q_{p0} = 21$.

DNS: 3D Stratified Forced Turbulence

A. Brandenburg, K. Kemel, N. Kleeorin, I. Rogachevskii, Astrophys. J. 749, 179 (2012)

$\mathrm{Rm} = \frac{u_{rms}}{\eta k_f} = 35; 70; 140;$ $\mathrm{Pm} = \frac{\nu}{\eta} = \frac{1}{4}; \frac{1}{2}; 1; 2; 4; 8;$ $k_f = (5 - 10)\, k_1$

$$\rho \frac{\mathrm{D}\boldsymbol{U}}{\mathrm{D}t} = \boldsymbol{J} \times \boldsymbol{B} - c_s^2 \boldsymbol{\nabla} \ln \rho + \boldsymbol{\nabla} \cdot (2\nu\rho\boldsymbol{\mathsf{S}}) + \rho(\boldsymbol{f} + \boldsymbol{g}),$$

$$\frac{\partial \boldsymbol{A}}{\partial t} = \boldsymbol{U} \times \boldsymbol{B} + \eta \nabla^2 \boldsymbol{A},$$

$$\frac{\partial \rho}{\partial t} = -\boldsymbol{\nabla} \cdot \rho \boldsymbol{U},$$

$$\boldsymbol{B} = \boldsymbol{B}_0 + \boldsymbol{\nabla} \times \boldsymbol{A}$$

$$\frac{\rho_{bot}}{\rho_{top}} = 535;$$

BOUNDARY CONDITIONS at the top and bottom:

$$U_z = 0, \quad \nabla_z U_x = \nabla_z U_y = 0$$
$$B_z = 0, \quad \nabla_z B_x = \nabla_z B_y = 0$$

BOUNDARY CONDITIONS:

1). The horizontal boundaries are periodic.

2). For the velocity we apply impenetrable, stress-free conditions.

3). For the magnetic field we use perfect conductor boundary conditions.

Effective Lorentz Force - DNS

$$\mathbf{F}^{\mathrm{eff}} = -\frac{1}{2}\nabla(1-q_p)\bar{\mathbf{B}}^2 + (\bar{\mathbf{B}}\cdot\nabla)(1-q_s)\bar{\mathbf{B}}$$

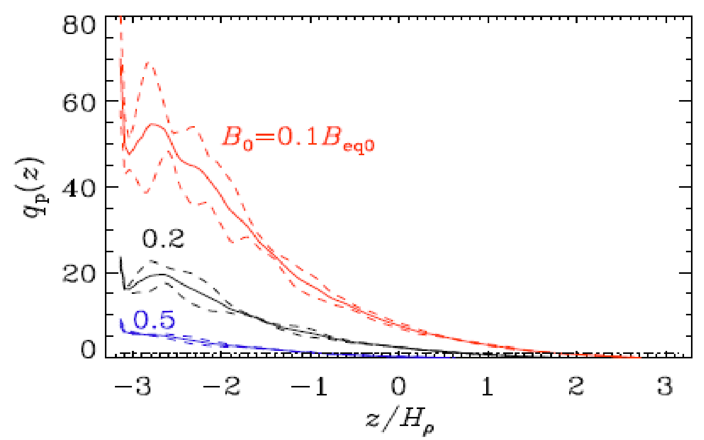

We perform horizontal averages which show a strong dependence on height:

$$\langle b_i b_j \rangle, \quad \langle u_i u_j \rangle,$$

We also perform time averaging in order to improve the statistics.

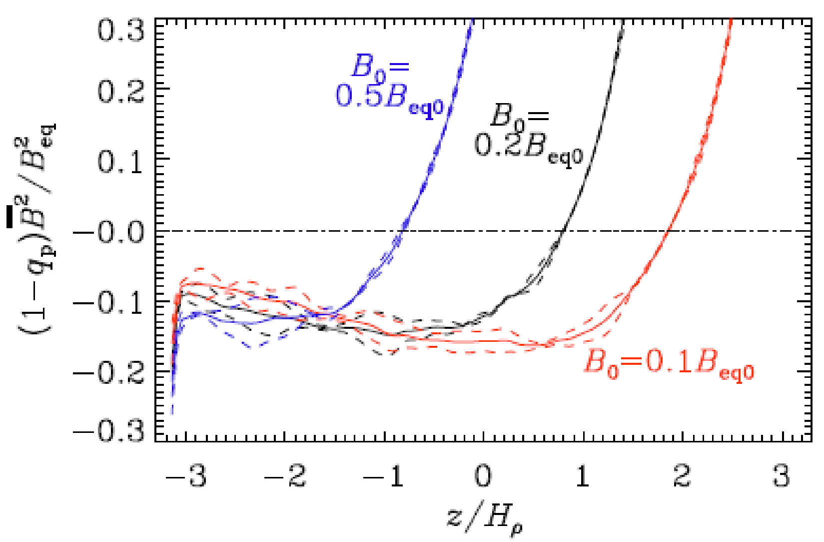

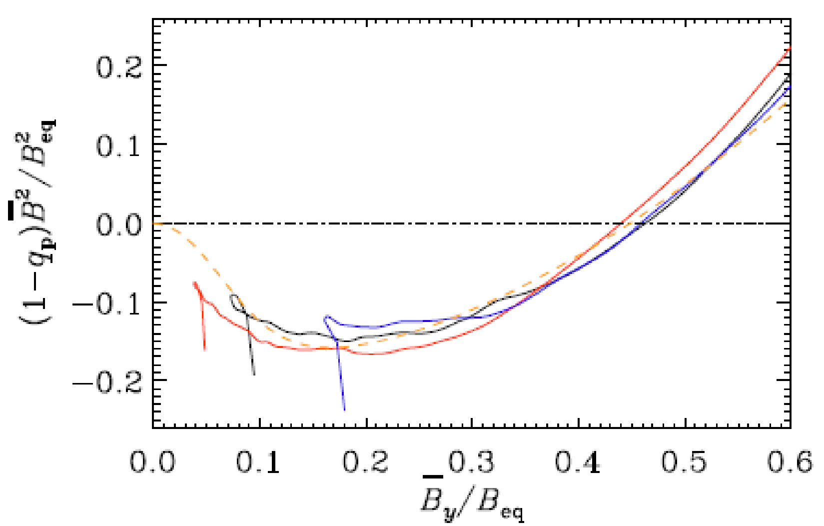

DNS: 3D Turbulent Convection

P. Käpulä, A. Brandenburg, N. Kleeorin, M. Mantere, I. Rogachevskii,
MNRAS, 422, 2465-2473 (2012)

$$\frac{\partial \boldsymbol{A}}{\partial t} = \boldsymbol{U} \times \boldsymbol{B} - \eta\mu_0 \boldsymbol{J},$$

$$\frac{D\ln\rho}{Dt} = -\boldsymbol{\nabla}\cdot\boldsymbol{U},$$

$$\frac{D\boldsymbol{U}}{Dt} = -\frac{1}{\rho}\boldsymbol{\nabla}p + \boldsymbol{g} + \frac{1}{\rho}\boldsymbol{J}\times\boldsymbol{B} + \frac{1}{\rho}\boldsymbol{\nabla}\cdot 2\nu\rho\mathbf{S},$$

$$\frac{De}{Dt} = -\frac{p}{\rho}\boldsymbol{\nabla}\cdot\boldsymbol{U} + \frac{1}{\rho}\boldsymbol{\nabla}\cdot K\boldsymbol{\nabla}T + 2\nu\mathbf{S}^2 + \frac{\mu_0\eta}{\rho}\boldsymbol{J}^2,$$

$$\boldsymbol{B} = \boldsymbol{B}_0 + \boldsymbol{\nabla}\times\boldsymbol{A}$$

$$\mathrm{Re} = \frac{u_{rms}\, d}{2\pi\,\nu} = 40 - 100\,,$$

$$\mathrm{Rm} = \frac{u_{rms}\, d}{2\pi\,\eta} = 10 - 50\,,$$

$$L_x = L_y = 5L_z = 5d; \quad (L_x = 10d) \qquad \frac{\rho_{bot}}{\rho_{top}} = 300;$$

BOUNDARY CONDITIONS:

$$U_z = 0, \quad \nabla_z U_x = \nabla_z U_y = 0$$
$$B_z \neq 0, \quad B_x = B_y = 0$$

BOUNDARY CONDITIONS:

1).The horizontal boundaries are periodic.

2). We keep the temperature fixed at the top and bottom boundaries.

3) For the velocity we apply impenetrable, stress-free conditions.

4). For the magnetic field we use vertical field conditions.

Effective Lorentz Force DNS: Turbulent Convection

$$\mathbf{F}^{\mathrm{eff}} = -\frac{1}{2}\nabla(1-q_p)\bar{\mathbf{B}}^2 + (\bar{\mathbf{B}}\cdot\nabla)(1-q_s)\bar{\mathbf{B}}$$

We perform horizontal averages which show a strong dependence on height.

We also perform time averaging in order to improve the statistics.

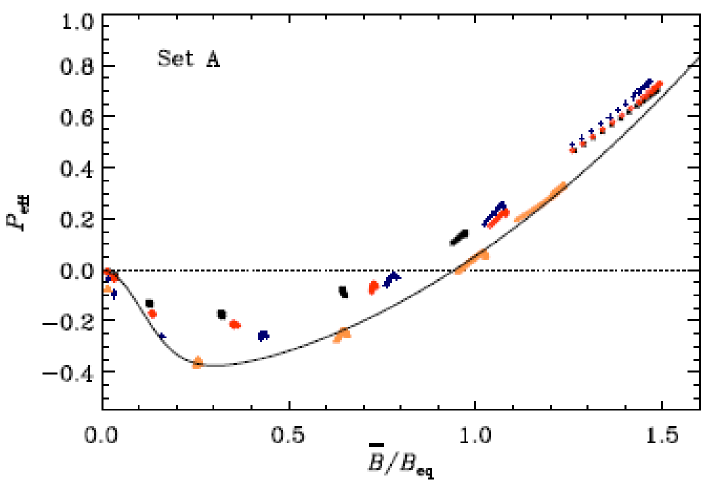

Figure 2. Effective magnetic pressure as a function of the mean magnetic field from weakly stratified Runs A1–A29 with an imposed horizontal field $\boldsymbol{B}_0 = B_0\hat{\boldsymbol{x}}$. The black stars, red diamonds, blue crosses, and yellow triangles denote simulations with Rm $\approx$ 10, 20, 50, and 70, respectively. We omit points near the boundaries at $z/d < 0.35$ and $z/d > 0.65$. The dashed and dotted lines correspond to approximate fits determined by Eq. (30), with $q_{p0} = 35$ and $B_p = 0.2B_{\mathrm{eq}}$, respectively.

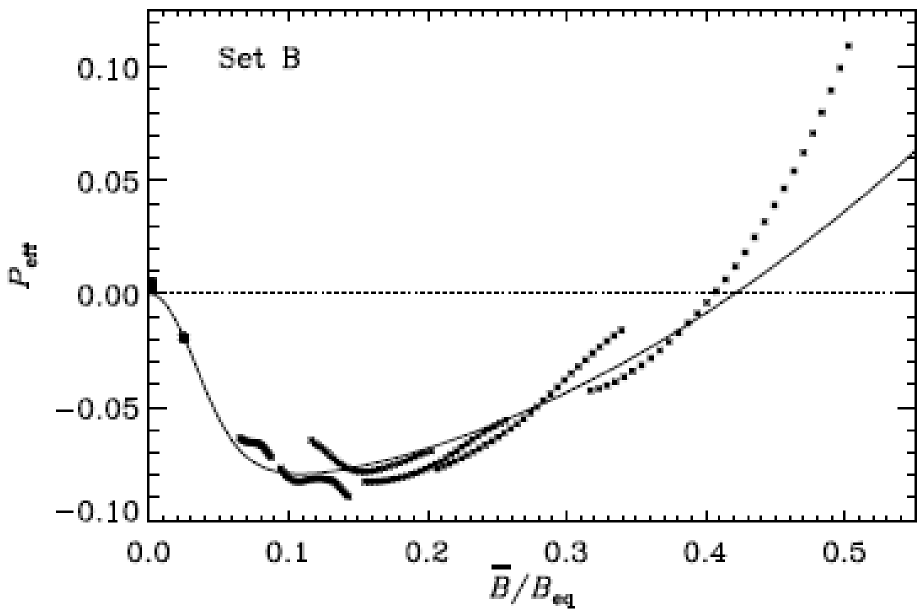

Figure 3. Same as Figure 2 but for Runs B1–B8 for Rm $=$ 40–50. The solid line corresponds to a fit with $q_{p0} = 70$ and $B_p = 0.063B_{\mathrm{eq}}$

Formation and Destruction of Bipolar Magnetic Structures

J. Warnecke, I.R. Losada, A. Brandenburg, N. Kleeorin and I. Rogachevskii,
Astrophys. J. Lett., 777, L37 (2013); Astron. Astrophys., submitted (2015)

Imposed horizontal field.

$$k_f = 30\, k_1;$$

BOUNDARY CONDITIONS at the top and bottom:

$$U_z = 0, \quad \nabla_z U_x = \nabla_z U_y = 0$$

But

$$z = -\pi:$$

$$B_z = 0, \quad \nabla_z B_x = \nabla_z B_y = 0$$

$$z = 2\pi:$$

$$B_x = B_y = 0.$$

Re=40, $\mathrm{Pr}_M = 0.06 - 1$

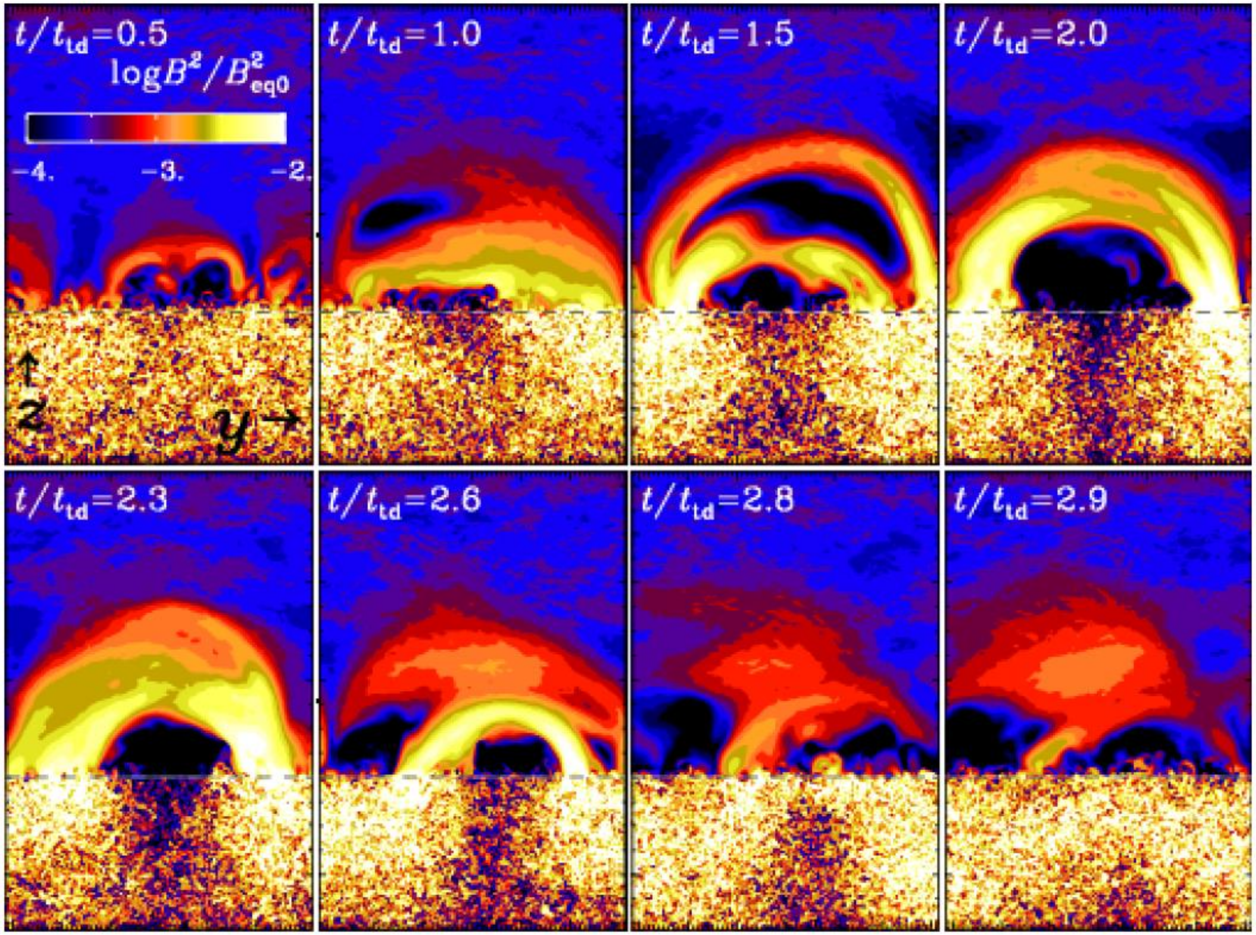

FIG. 5.— Time series of B^2/B^2_{eq0} in a vertical cut through the bipolar region at $x = 0$. Note the y axis is shifted the see the formation of the loop.

Formation and Destruction of Bipolar Magnetic Structures

J. Warnecke, I.R. Losada, A. Brandenburg, N. Kleeorin and I. Rogachevskii,

Astroph. J. Lett. 777, L37 (2013); Astron. Astoph., submitted (2015).

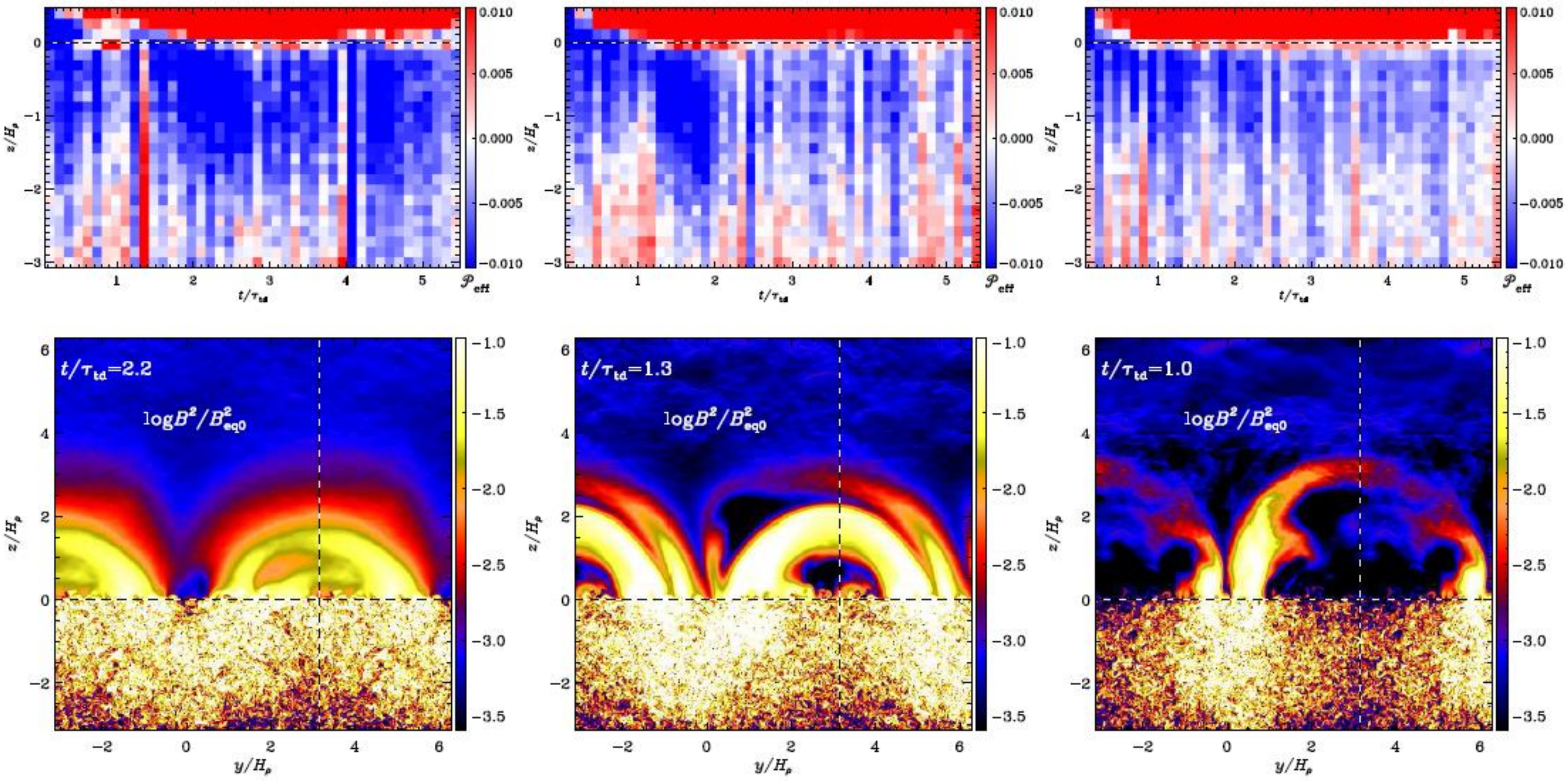

Fig. 2. Formation of bipolar regions for three different stratifications (left column: A3, middle: A5, right: A7). *Top row:* normalized vertical magnetic field $B_z/B_{\rm eq0}$ plotted at the xy surface ($z = 0$) at times, when the bipolar regions are the clearest. *Middle top row:* vertical rms magnetic field $B_z^{\rm rms}/B_{\rm eq} = \langle B_z^2\rangle_{xy}/B_{\rm eq}$ normalized by the local equipartition value as a function of time $t/\tau_{\rm td}$ and height z. *Middle bottom row:* rebined effective magnetic pressure $\mathcal{P}_{\rm eff}$ as a function of time $t/\tau_{\rm td}$ and height z. Blue shades correspond to negative and red to positive values. *Bottom row:* normalized magnetic energy density plotted in the yz plane as a vertical cut through the bipolar region at $x = 0$. The domain has been replicated by 50% in the y direction to give a more complete impression about spot separation and arch length. The black-white dashed lines marks the replicated part and in the last three rows the the surface ($z = 0$).

DNS: The Result is Robust

$$\mathcal{P}_{\rm eff} = \frac{1}{2}(1 - q_p)\frac{\bar{\rm B}^2}{{\rm B}_{\rm eq}^2}$$

Effect does not exist only below $\mathrm{Rm} = 1$

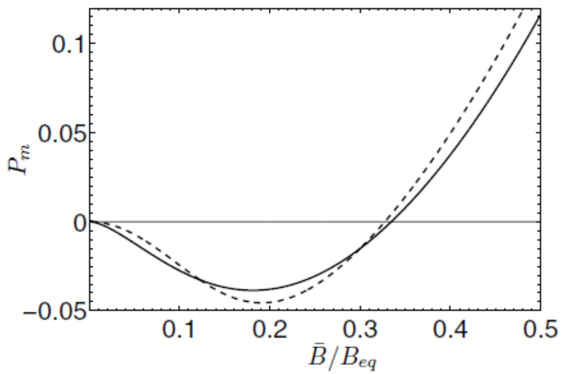

Fig. 3 The effective mean magnetic pressure $P_m(\overline{B}) = (1 - q_{\rm p})\overline{B}^2/\overline{B}_{\rm p}^2$ determined by Rogachevskii & Kleeorin (2007) – solid line, and by the model described by Eq. (26) – dashed line ($\overline{B}_{\rm p} = 0.21\, c_{s0}\rho_0^{1/2}$ and $q_{\rm p0} = 4$).

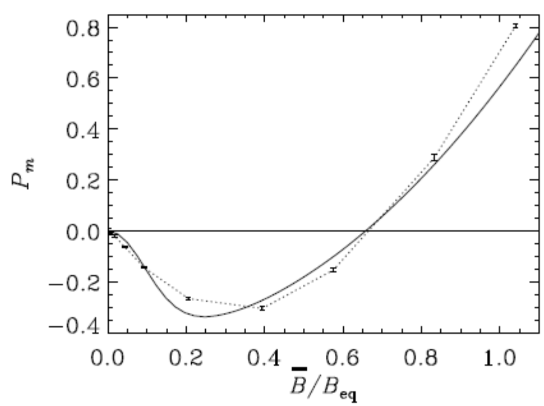

Fig. 4 Same as Fig. 3, but from simulation (dotted line). The solid line shows a fit [Eq. (26)] with $\overline{B}_{\rm p} = 0.022\, c_{s0}\rho_0^{1/2}$ (corresponding to $\overline{B}_{\rm p}/B_{\rm eq} = 0.18$) and $q_{\rm p0} = 21$.

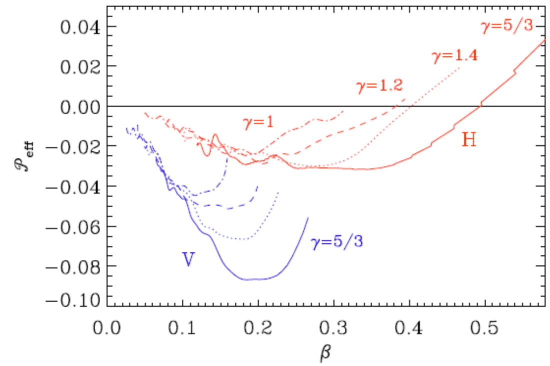

Fig. 7. Effective magnetic pressure obtained from DNS in a polytropic layer with different γ for horizontal (H, red curves) and vertical (V, blue curves) mean magnetic fields.

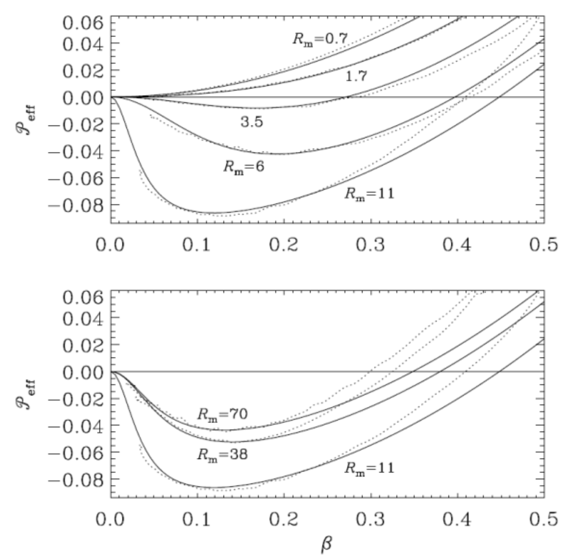

Figure 7. Normalized effective magnetic pressure, $\mathcal{P}_{\rm eff}(\beta)$, for low (upper panel) and higher (lower panel) values of Re_M. The solid lines represent the fits to the data shown as dotted lines.

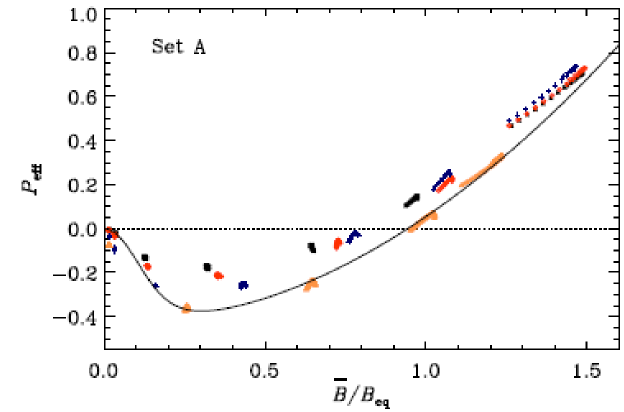

Figure 2. Effective magnetic pressure as a function of the mean magnetic field from weakly stratified Runs A1–A29 with an imposed horizontal field $\boldsymbol{B}_0 = B_0\hat{\boldsymbol{x}}$. The black stars, red diamonds, blue crosses, and yellow triangles denote simulations with Rm $\approx$ 10, 20, 50, and 70, respectively. We omit points near the boundaries at $z/d < 0.35$ and $z/d > 0.65$. The dashed and dotted lines correspond to approximate fits determined by Eq. (30), with $q_{p0} = 35$ and $B_p = 0.2B_{\rm eq}$, respectively.

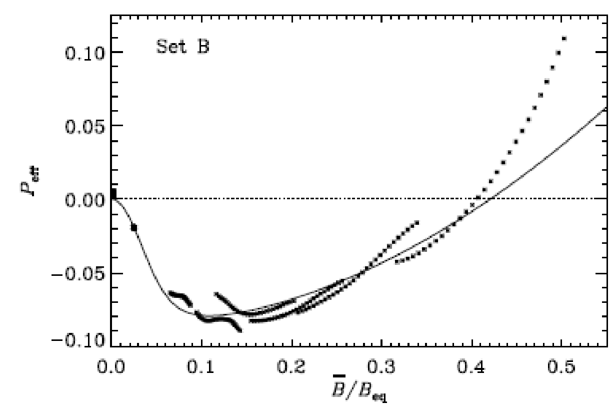

Figure 3. Same as Figure 2 but for Runs B1–B8 for Rm $=$ 40–50. The solid line corresponds to a fit with $q_{p0} = 70$ and $B_p = 0.063B_{\rm eq}$

NEMPI in DNS: 3D Forced Turbulence (Horizontal imposed weak magnetic field)

A. Brandenburg, K. Kemel, N. Kleeorin, Dh. Mitra, and I. Rogachevskii, Astrophys. J. Lett. 740, L50 (2011); Solar Phys. 280, 321-333 (2012).

$$\rho \frac{\mathrm{D}\boldsymbol{U}}{\mathrm{D}t} = -c_s^2 \boldsymbol{\nabla}\rho + \boldsymbol{J} \times \boldsymbol{B} + \rho(\boldsymbol{f} + \boldsymbol{g}) + \boldsymbol{\nabla} \cdot (2\nu\rho \mathsf{S}),$$

$$\frac{\partial \boldsymbol{A}}{\partial t} = \boldsymbol{U} \times \boldsymbol{B} + \eta \nabla^2 \boldsymbol{A},$$

$$\frac{\partial \rho}{\partial t} = -\boldsymbol{\nabla} \cdot \rho \boldsymbol{U},$$

$$\boldsymbol{B} = \boldsymbol{B}_0 + \boldsymbol{\nabla} \times \boldsymbol{A}$$

$$\mathrm{Rm} = \frac{u_{rms}}{\eta k_f} = 35; 70; 140;$$

$$\mathrm{Pm} = \frac{\nu}{\eta} = \frac{1}{4}; \frac{1}{2}; 1; 2; 4; 8;$$

$$k_f = (5 - 30)\, k_1;$$

$$\frac{\rho_{bot}}{\rho_{top}} = 535;$$

BOUNDARY CONDITIONS at the top and bottom:

$$U_z = 0, \quad \nabla_z U_x = \nabla_z U_y = 0$$

$$B_z = 0, \quad \nabla_z B_x = \nabla_z B_y = 0$$

BOUNDARY CONDITIONS:

1).The horizontal boundaries are periodic.

2). For the velocity we apply impenetrable, stress-free conditions.

3). For the magnetic field we use perfect conductor boundary conditions.

DNS: 3D Stratified Forced Turbulence

Visualizations of horizontal magnetic field

$$k_f = 30\, k_1$$

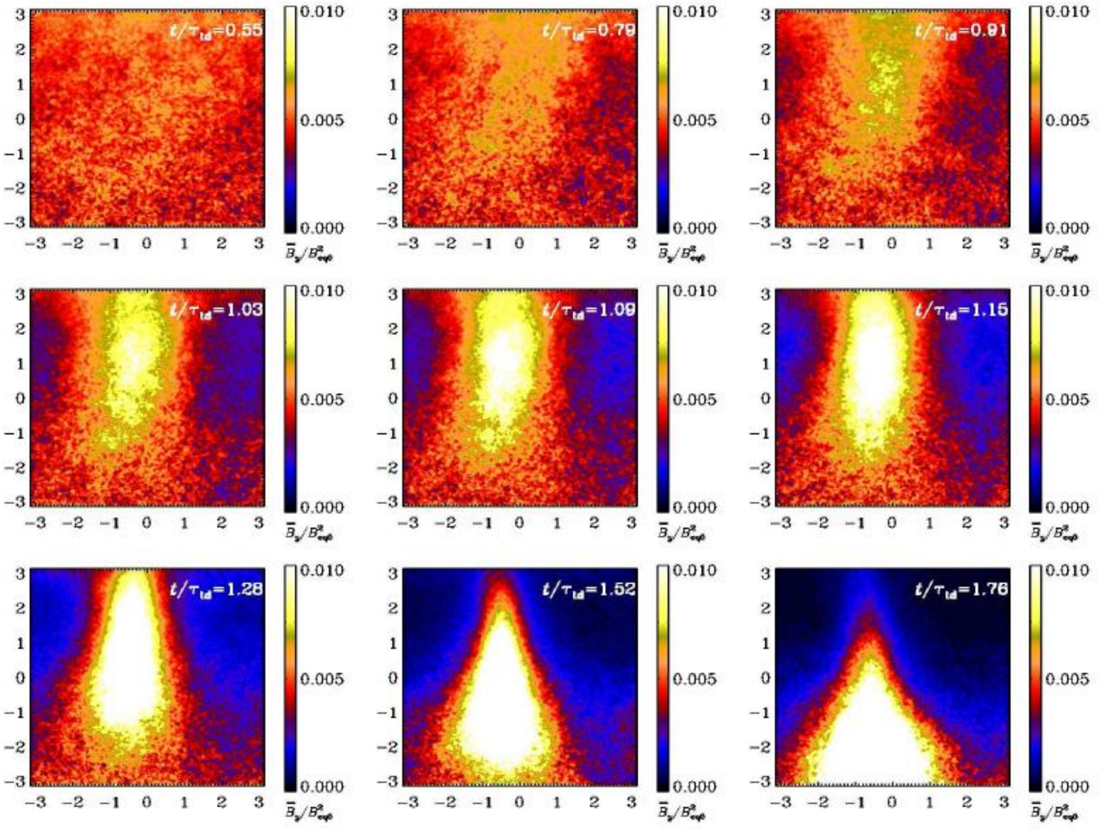

Figure 1. Visualizations of $\overline{B}_y(x,z,t)$ for different times. Time is indicated in turbulent diffusive times, $(\eta_{t0}k_1^2)^{-1}$, corresponding to about 5000 turnover times, i.e., $t = 5000/u_{\rm rms}k_{\rm f}$. $\mathrm{Re}_M = 18$ and $\mathrm{Pr}_M = 0.5$.

$$P_{\rm tot} = \rho T + (1-q_p)\frac{\overline{\mathrm{B}}^2}{2}$$

A. Brandenburg, K. Kemel, N. Kleeorin, Dh. Mitra, and I. Rogachevskii, Astrophys. J. Lett. 740, L50 (2011); Solar Phys. 280, 321-333 (2012).

DNS: 3D Stratified Forced Turbulence

Formation of magnetic structures from initially uniform horizontal field

$k_f = 30\, k_1$

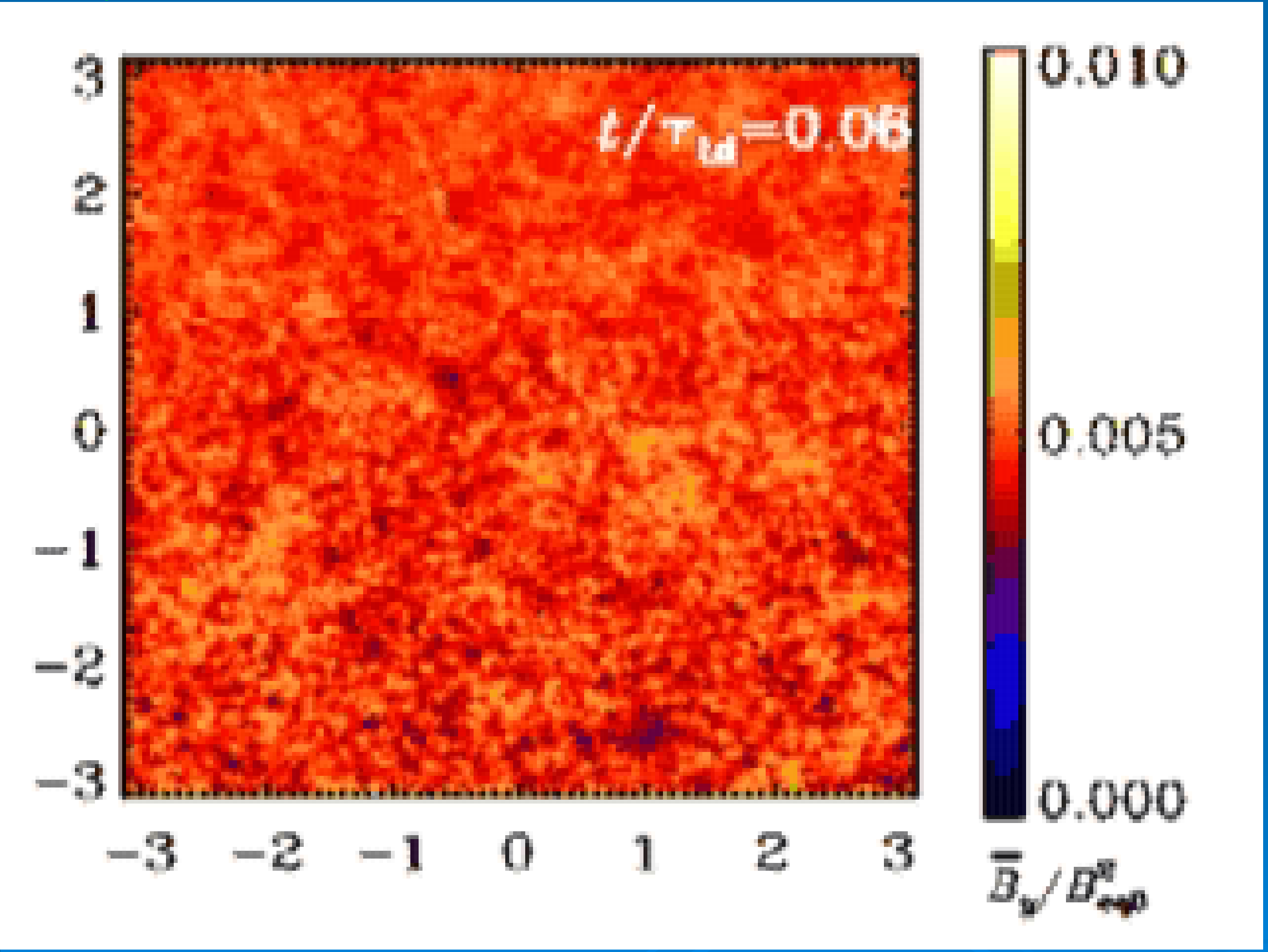

Potato-Sack Effect

1. During the first 500 turnover times, flux concentrations form first near the surface.
2. At later times the location of the peak magnetic field moves gradually downward.
3. This phenomenon is a direct consequence of the negative effective magnetic pressure, making such structures heavier than their surroundings.

$$P_{\rm tot} = \rho T + (1 - q_p)\frac{\bar{\rm B}^2}{2}$$

A. Brandenburg, K. Kemel, N. Kleeorin, Dh. Mitra, and I. Rogachevskii, Astrophys. J. Lett. 740, L50 (2011); Solar Phys. 280, 321-333 (2012).

Large-Scale MHD-Instability (NEMPI)

A. Brandenburg, K. Kemel, N. Kleeorin, Dh. Mitra, and I. Rogachevskii,
Astrophys. J. Lett. 740, L50 (2011); Solar Phys. 280, 321-333 (2012).

Slow growth

$$\lambda = \frac{v_A}{H_\rho}\left(-2\frac{\mathrm{d}\mathcal{P}_{\mathrm{eff}}}{\mathrm{d}\beta^2}\right)^{1/2}\frac{k_x}{k}.$$

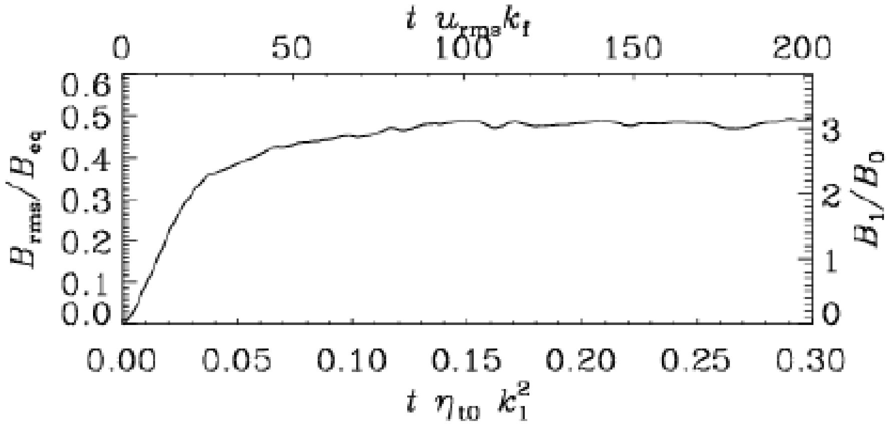

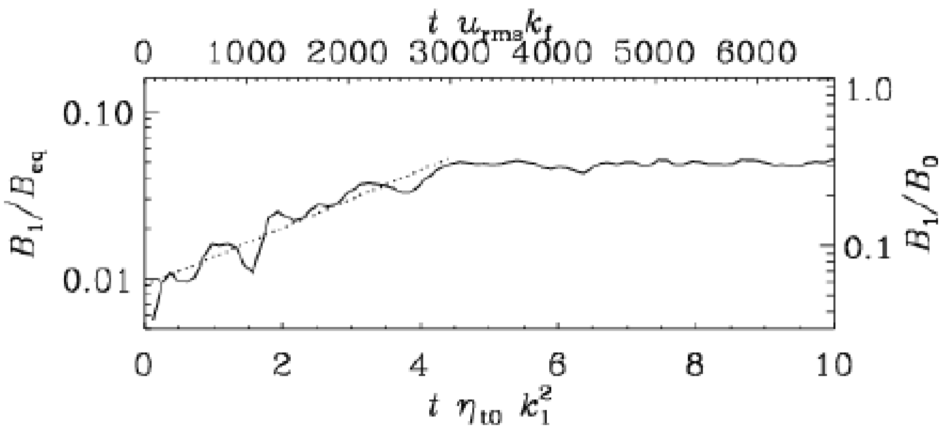

- Several thousand turnover times
- Or ½ a turbulent diffusive time
- Exponential growth → linear instability of an already turbulent state

Large-Scale MHD-Instability

Let us estimate the growth rate of this instability. Neglecting dissipative processes for simplicity's sake, we shall retain only the Archimedes force in the momentum equation of the magnetic flux tube

$$\frac{d^2\zeta}{dt^2} = -\left(\frac{C_A}{C_s}\right)^2 \frac{gQ_p(L_B - L_\rho)}{L_B L_\rho}\zeta \ ,$$

where $C_A = \bar{B}a/\sqrt{\mu\rho a}$ is the Alfven velocity. The growth rate of this instability is given by

$$\gamma \simeq \frac{C_A}{L_\rho}\left[Q_p\left(\frac{L_\rho}{L_B} - 1\right)\right]^{1/2} \ .$$

Here $L_\rho \simeq C_s^2/g$.

NEMPI in DNS: 3D Forced Turbulence
(Vertical Imposed Weak Magnetic Field)

All simulations are performed with the PENCIL CODE, that uses sixth-order explicit finite differences in space and a third-order accurate time stepping method.

$$\rho\frac{\mathrm{D}\boldsymbol{U}}{\mathrm{D}t} = -c_\mathrm{s}^2\boldsymbol{\nabla}\rho + \boldsymbol{J}\times\boldsymbol{B} + \rho(\boldsymbol{f}+\boldsymbol{g}) + \boldsymbol{\nabla}\cdot(2\nu\rho\mathsf{S}),$$

$$\frac{\partial\boldsymbol{A}}{\partial t} = \boldsymbol{U}\times\boldsymbol{B} + \eta\nabla^2\boldsymbol{A},$$

$$\frac{\partial\rho}{\partial t} = -\boldsymbol{\nabla}\cdot\rho\boldsymbol{U},$$

$$B = B_0 + \nabla \times A$$

$$\mathrm{Rm} = \frac{u_{rms}}{\eta\, k_f} = 18\, \mathbf{, 40, 95}$$

$$\mathrm{Pm} = \frac{\nu}{\eta} = \frac{1}{2}$$

$$k_f = 30\, k_1;$$

$$\frac{\rho_{bot}}{\rho_{top}} = 535;$$

BOUNDARY CONDITIONS
at the top and bottom:

$$U_z = 0, \quad \nabla_z U_x = \nabla_z U_y = 0$$

$$B_x = B_y = 0,$$

BOUNDARY CONDITIONS:

1). The horizontal boundaries are periodic.

2). For the velocity we apply impenetrable, stress-free conditions.

3). For the magnetic field we use vertical field boundary conditions.

Formation of Magnetic Spots in DNS

(Vertical Imposed Weak Magnetic Field)

PENCIL CODE $256^3; 512^3; 1024^3$

$k_f = 30\,k_1;$

$\mathrm{Rm} = \frac{u_{rms}}{\eta\,k_f} = 18; 40; 95$

$\mathrm{Pm} = \frac{\nu}{\eta} = \frac{1}{2}$

$\frac{\rho_{bot}}{\rho_{top}} = 535;$

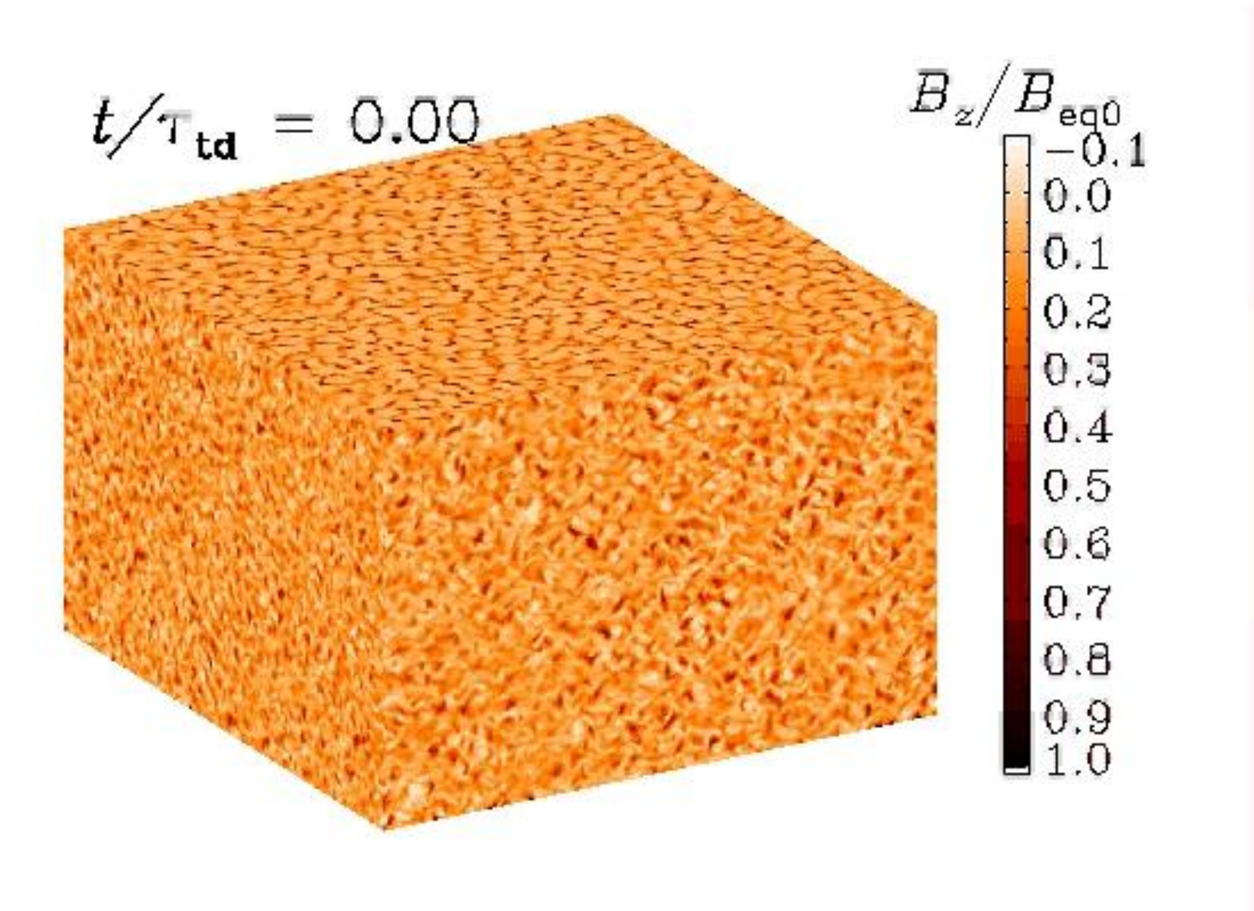

BOUNDARY CONDITIONS at the top and bottom:

1. stress-free conditions
$\nabla_z U_x = \nabla_z U_y = 0$
$U_z = 0,$
2. vertical field
$B_x = B_y = 0,$

A. Brandenburg, N. Kleeorin and I. Rogachevskii, Astrophys. J. Lett., 776, L23 (2013)

Time-evolution of the Magnetic Spot

A. Brandenburg, N. Kleeorin and I. Rogachevskii, Astrophys. J. Lett., 776, L23 (2013)

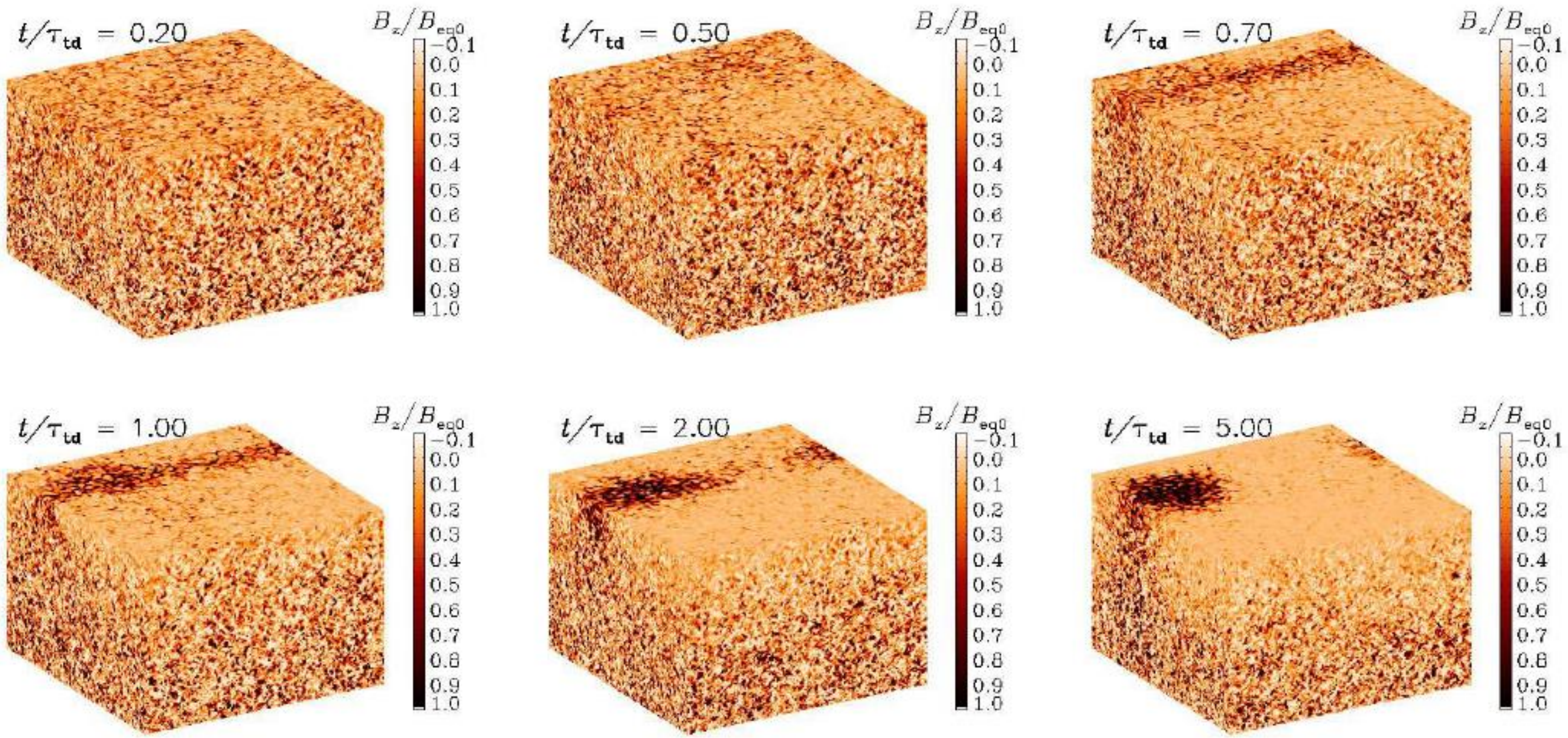

FIG. 1.— Evolution from a statistically uniform initial state toward a single spot for $B_{z0}/B_{eq0} = 0.02$. Here, B_z/B_{eq0} is shown on the periphery of the domain. Dark shades correspond to strong vertical fields. Time is in units of τ_{td}.

Structure of the Magnetic Spot

A. Brandenburg, N. Kleeorin and I. Rogachevskii, Astrophys. J. Lett., 776, L23 (2013)

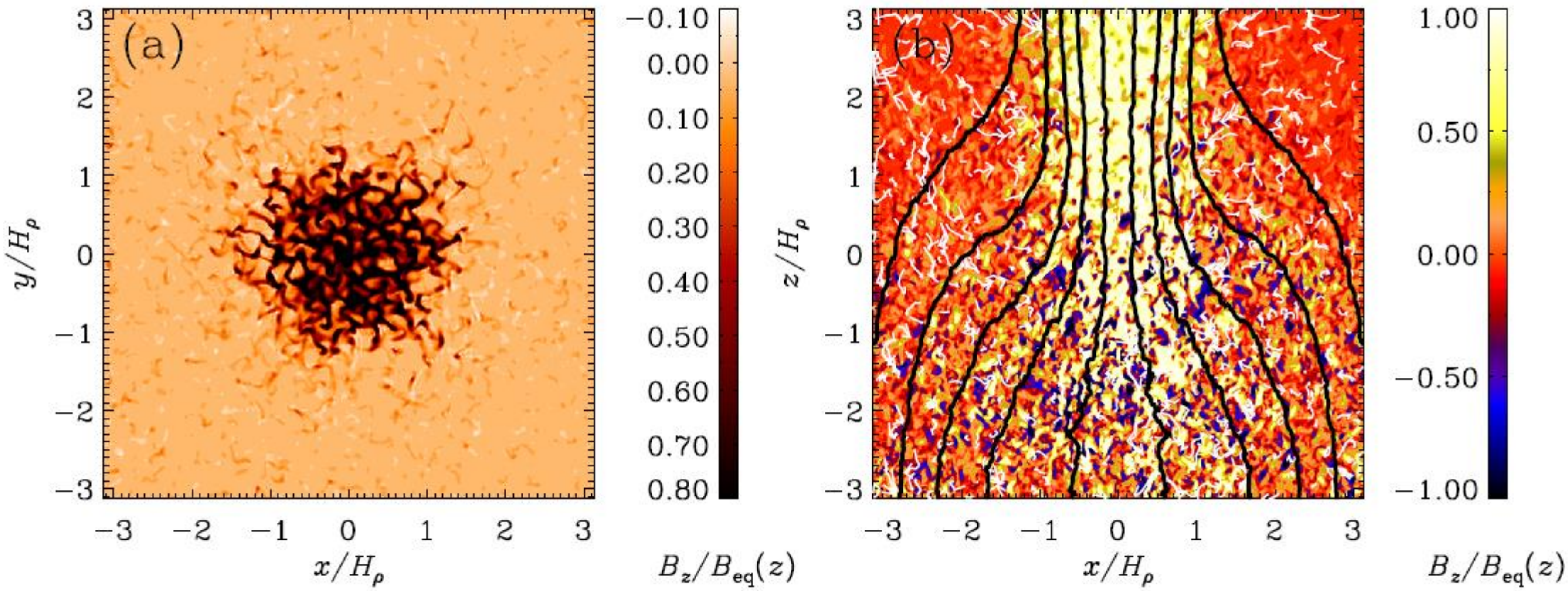

FIG. 3.— Cuts of $B_z/B_{\rm eq}(z)$ in the xy plane at the top boundary ($z/H_\rho = \pi$) and the xz plane through the middle of the spot at $y = 0$. In the xz cut, we also show magnetic field lines and flow vectors obtained by numerically averaging in azimuth around the spot.

Linear Phase of NEMPI

A. Brandenburg, N. Kleeorin and I. Rogachevskii, **Astrophys. J. Lett., 776, L23 (2013)**

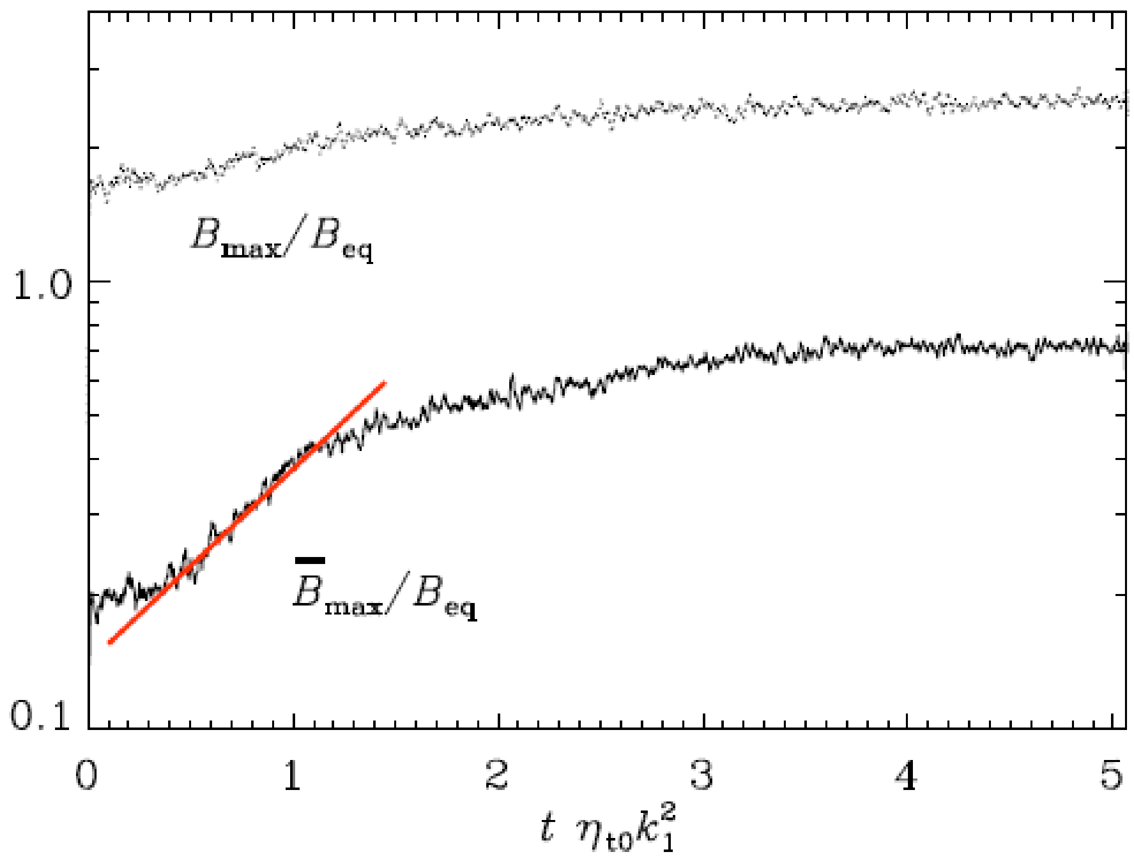

FIG. 2.— Growth of $\overline{B}_{max}/B_{eq}$ (solid line) and B_{max}/B_{eq} (dotted line) at the top of the domain. The straight red line gives a fit to $\overline{B}_{max}/B_{eq}$ with a slope of unity corresponding to the growth rate $(\eta_{t0}k_1^2)^{-1}$.

Formation of Magnetic Spots in DNS
(Vertical Imposed Weak Magnetic Field)

A. Brandenburg, N. Kleeorin and I. Rogachevskii, Astrophys. J. Lett., 776, L23 (2013)

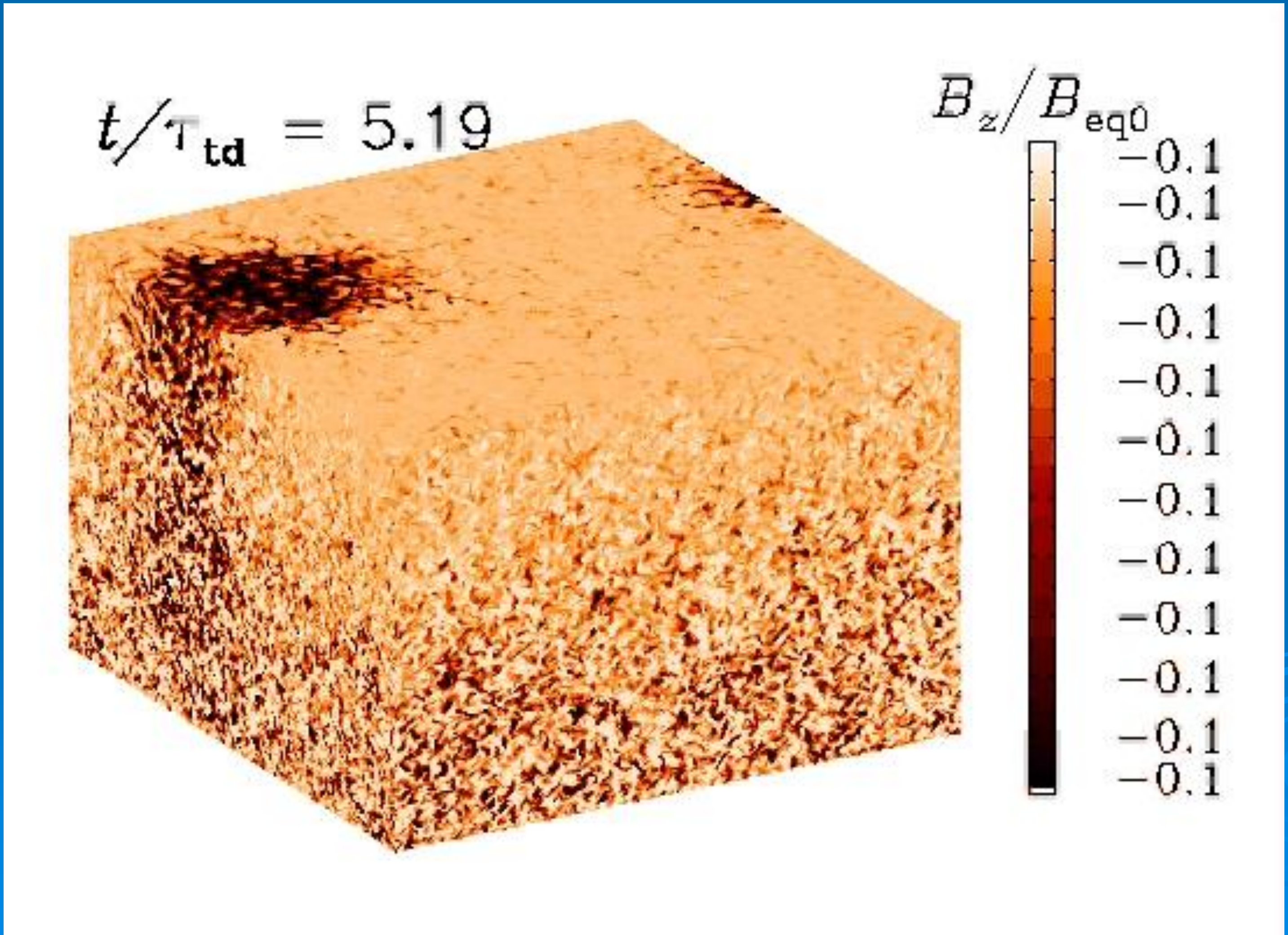

1024^3

NEMPI is the Large-Scale Instability

A. Brandenburg, O. Gressel, S. Jabbari, N. Kleeorin, I. Rogachevskii,
Astron. Astrophys. 562, A53 (2014).

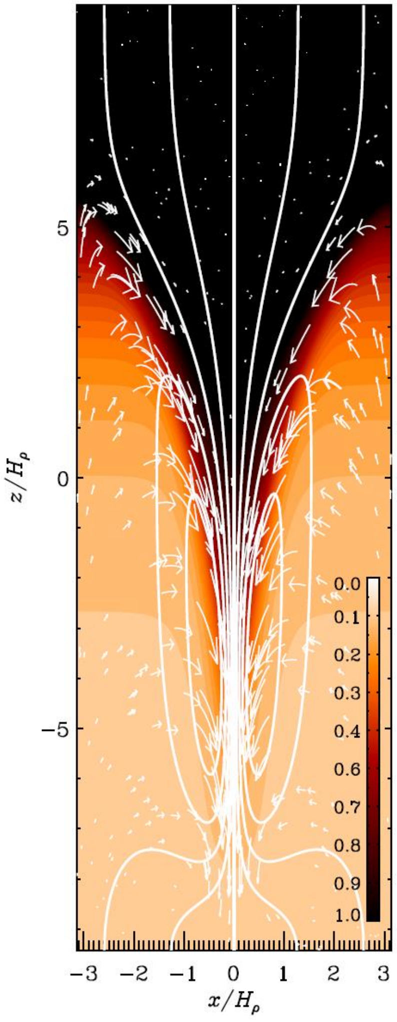

Fig. 5. $\overline{B}_z/B_{\rm eq}$ together with field lines and flow vectors from MFS, for Run Bv05/33 with $B_0/B_{\rm eq0} = 0.05$. The flow speed varies from $-0.27u_{\rm rms}$ (downward) to $0.08u_{\rm rms}$ (upward).

1. A local increase of the magnetic field causes a decrease of the negative effective magnetic pressure.
2. This is compensated for by enhanced gas pressure, leading to enhanced gas density, so the gas is heavier than its surroundings and sinks.
3. This results in a positive feedback loop: downflow compresses the magnetic field, the effective magnetic pressure becomes more negative, gas pressure increases, so the density increases, and the downflow accelerates, and causes NEMPI.

$$P_{\rm tot} = \rho T + (1 - q_p)\frac{\overline{\mathbf{B}}^2}{2}$$

Simulations: DNS and MFS

Vertical Imposed Field in Polytropic Atmosphere

I.R. Losada, A. Brandenburg, N. Kleeorin, I. Rogachevskii,
Astron. Astrophys. 564, A2, (2014);

$$p(z) = \rho^{\gamma} \qquad \gamma = 5/3$$

DNS

MFS

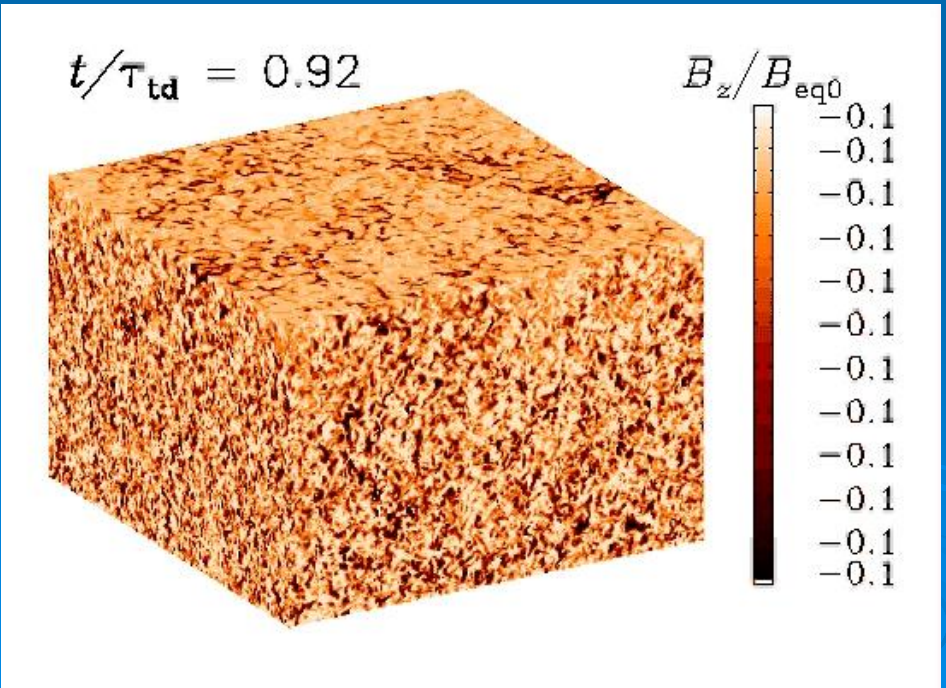

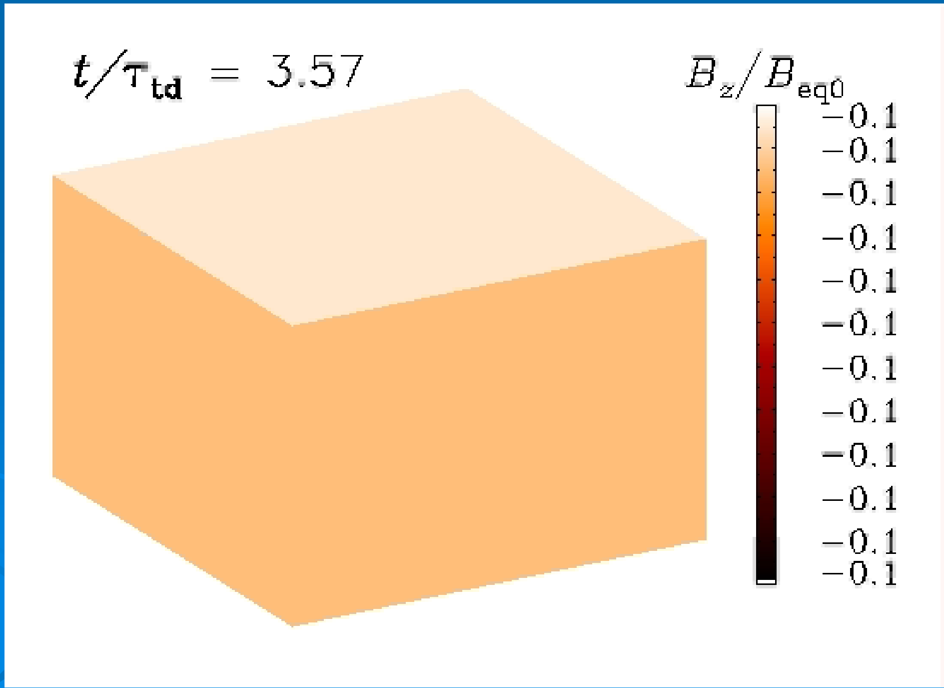

DNS and Mean-Field Simulations

$\gamma = 5/3$

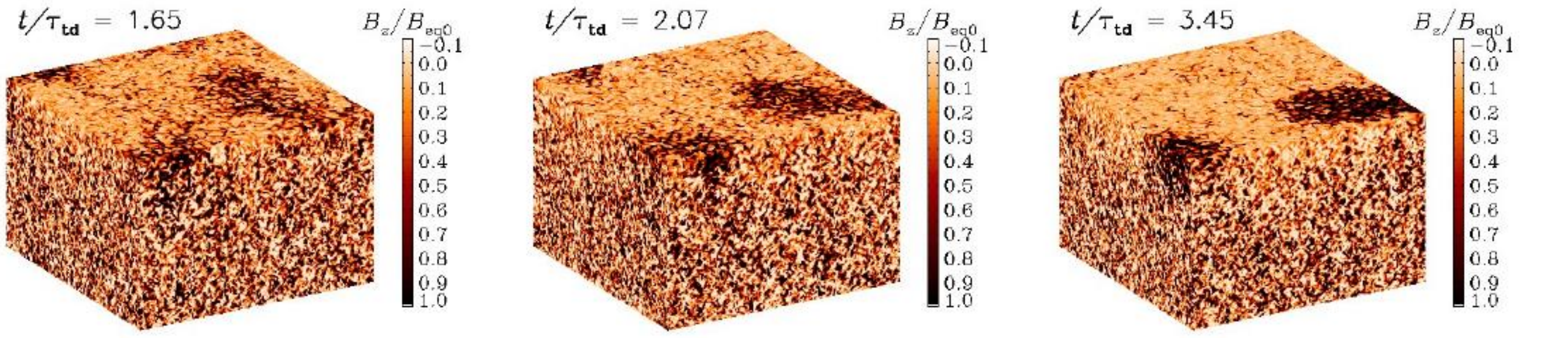

Fig. 5. Snapshots from DNS showing $\overline{B}_z$ on the periphery of the computational domain for $\gamma = 5/3$ and $\beta_0 = 0.05$ at different times for the case of a vertical field using the vertical field boundary condition.

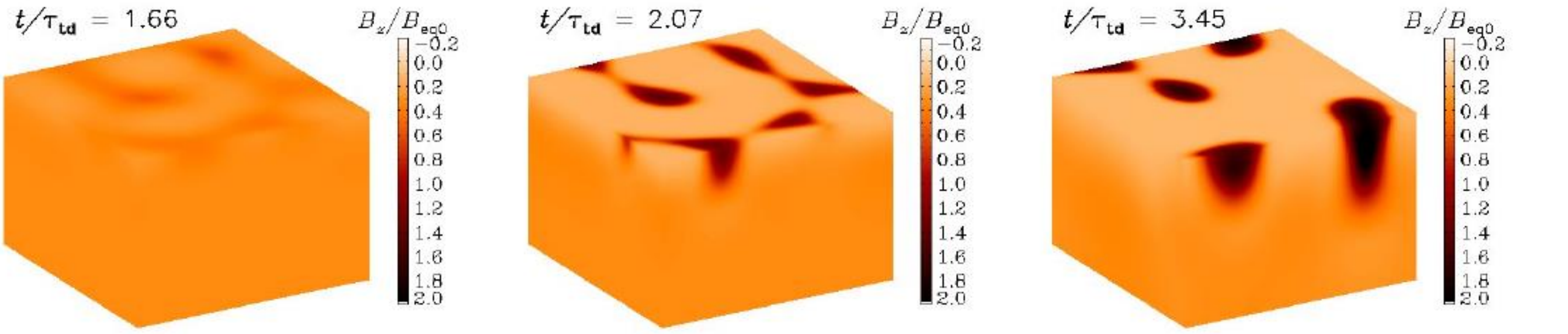

Fig. 17. Similar to Fig. 16 of MFS, but for Model II at times similar to those in the DNS of Fig. 5. Note that there are now more structures than in the earlier MFS of Fig. 16, and that they develop more rapidly.

Formation and Destruction of Bipolar Magnetic Structures

J. Warnecke, I.R. Losada, A. Brandenburg, N. Kleeorin and I. Rogachevskii,

Astrophys. J. Lett., 777, L37 (2013); Astron. Astrophys., submitted (2015)

Imposed horizontal field.

$$k_f = 30\, k_1;$$

BOUNDARY CONDITIONS at the top and bottom:

$$U_z = 0, \;\; \nabla_z U_x = \nabla_z U_y = 0$$

But

$$z = -\pi :$$

$$B_z = 0, \;\; \nabla_z B_x = \nabla_z B_y = 0$$

$$z = 2\pi :$$

$$B_x = B_y = 0.$$

Re=40, $\mathrm{Pr}_M = 0.06 - 1$

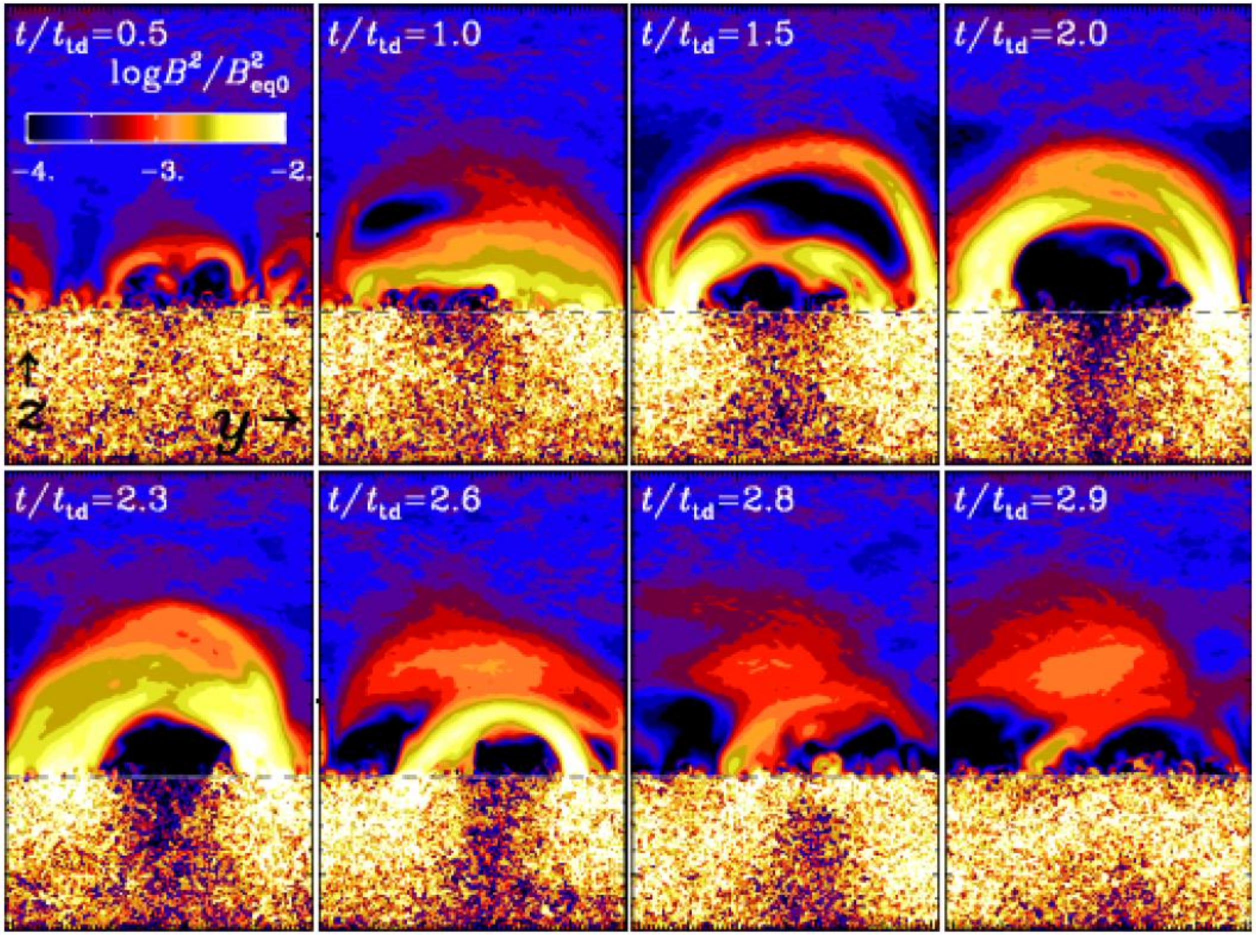

FIG. 5.— Time series of B^2/B^2_{eq0} in a vertical cut through the bipolar region at $x = 0$. Note the y axis is shifted the see the formation of the loop.

Formation and Destruction of Bipolar Magnetic Structures

J. Warnecke, I.R. Losada, A. Brandenburg, N. Kleeorin and I. Rogachevskii,
Astrophys. J. Lett., 777, L37 (2013); Astron. Astrophys., submitted (1015).

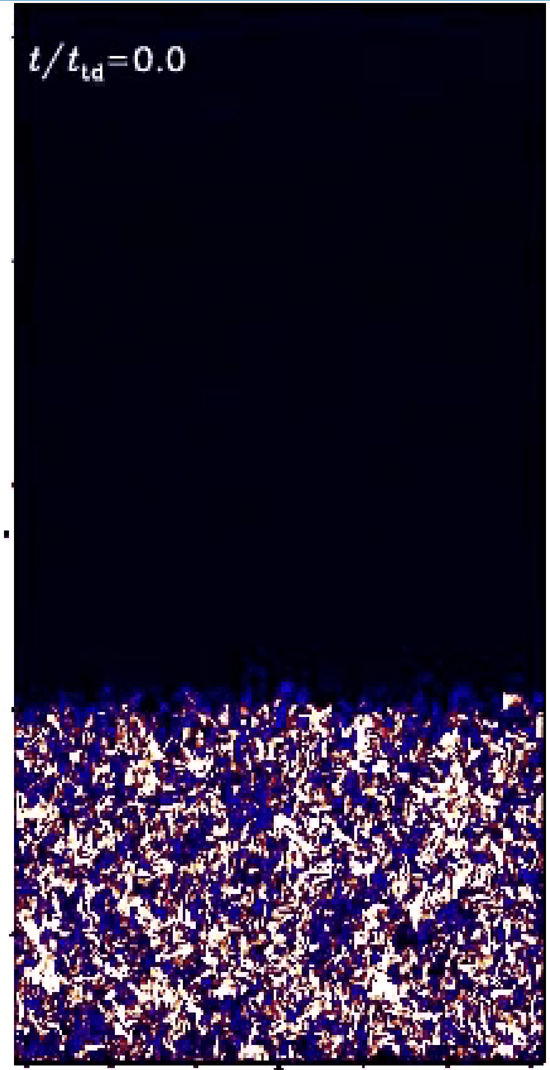

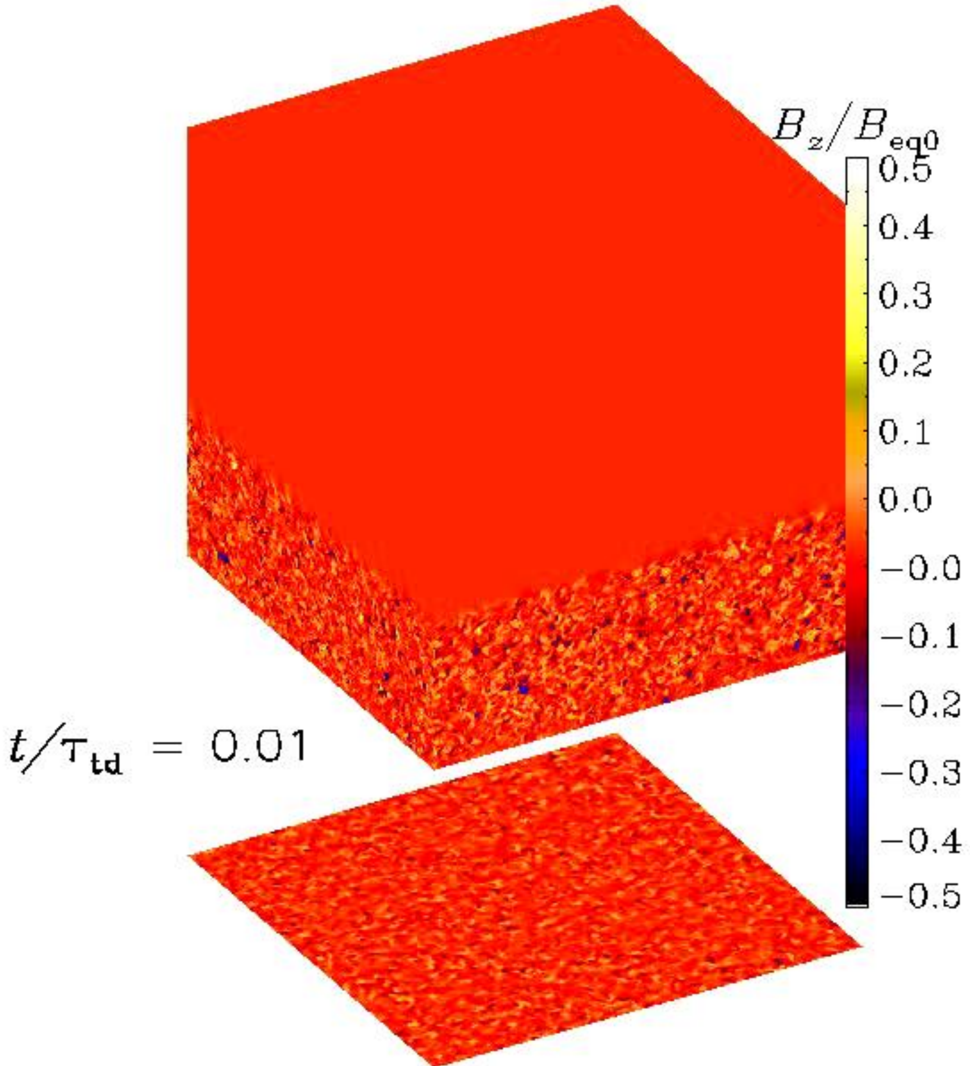

Magnetic Structures

J. Warnecke, I.R. Losada, A. Brandenburg, N. Kleeorin and I. Rogachevskii,

Astrophys. J. Lett., 777, L37 (2013), Astron. Astrophys., submitted (2015).

Simulations

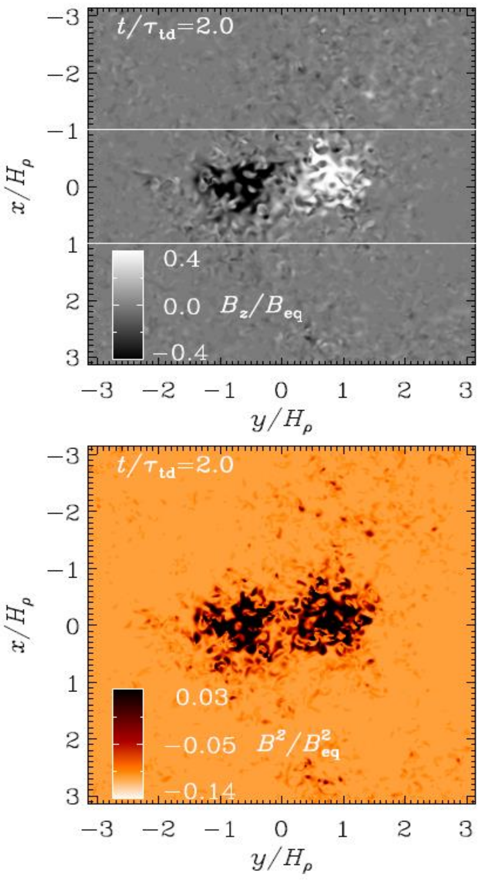

FIG. 1.— *Upper panel:* normalized vertical magnetic field B_z/B_{eq} of the bipolar region at the surface ($z = 0$) of the simulation domain. The white lines delineate the area shown in Figure 3. *Lower panel:* normalized magnetic energy B^2/B_{eq}^2 of the two regions relative to the rest of the surface. Note that we clip both color tables to increase the visualization of the structure. The field strength reaches around $B_z/B_{eq} = 1.4$.

Sunspots

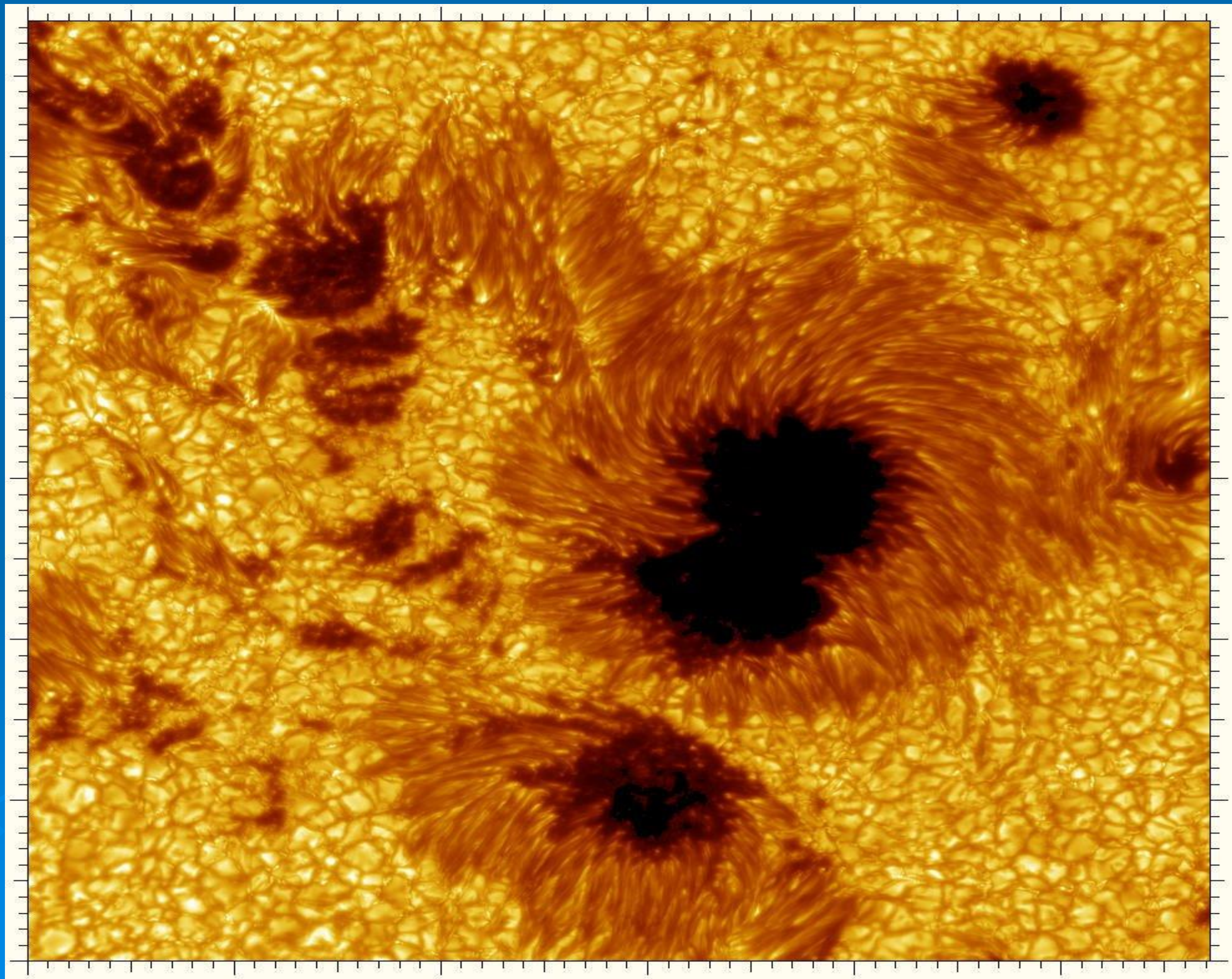

Parameters (top of Solar Convective Zone)

In the upper part of the convective zone, at depth depth $H \sim 10^9$ cm,

the magnetic Reynolds number $\mathrm{Rm} \sim 3 \times 10^7$,

the maximum scale of turbulent motions $l_0 \sim 2.8 \times 10^8$ cm,

the characteristic turbulent velocity in the maximum scale l_0 of turbulent motions $u_0 \sim 10^4$ cm s^{-1},

the turbulent magnetic diffusion $\eta_T \sim 10^{12}$ cm^2 s^{-1},

the equipartition mean magnetic field $\bar{B}_{\mathrm{eq}} = 700$ G.

the characteristic time of developing of the instability $T \sim 1.2$ days; the turbulent diffusion time $T_D \sim 12$ days; the critical magnetic field for the instability $\bar{B}_{\mathrm{cr}} = 0.03\bar{B}_{\mathrm{eq}}$.

Parameters (bottom of CZ)

The solar convective zone

At the base of the convective zone (at depth $H \sim 2 \times 10^{10}$ cm),

the magnetic Reynolds number $\mathrm{Rm} = l_0 u_0/\eta \sim 2 \cdot 10^9$,

the maximum scale of turbulent motions $l_0 \sim 8 \times 10^9$ cm,

the characteristic turbulent velocity $u_0 \sim 2 \times 10^3$ cm s^{-1},

the turbulent magnetic diffusion $\eta_T \sim 5.3 \times 10^{12}$ cm^{2}s^{-1},

the equipartition mean magnetic field $\bar{B}_{\mathrm{eq}} = 3000$ G.

the characteristic time of developing of the instability $T \sim 1$ year; the turbulent diffusion time $T_D \sim 3$ years; the critical magnetic field for the instability $\bar{B}_{\mathrm{cr}} = 0.1\bar{B}_{\mathrm{eq}}$.

Summary

- Generation of magnetic fluctuations in a turbulence with large plasma beta results in a strong reduction of the large-scale magnetic pressure, so that effective magnetic pressure (sum of turbulent and non-turbulent contributions) can be negative.
- This causes excitation of negative effective magnetic pressure instability (NEMPI) and formation of the large-scale magnetic structures even in originally uniform mean magnetic field.
- DNS of two-layer systems: non-helical forcing layer with external coronal envelope show that these magnetic inhomogeneties have bipolar structures which are broadly reminiscent of Sunspots and Active Regions.

THE END